Steel and Composite Structures, *Vol. 30, No. 6 (2019) 493-516*
DOI: https://doi.org/10.12989/scs.2019.30.6.493

Nonlinear vibration analysis of carbon nanotube reinforced composite plane structures

Mohammad Rezaiee-Pajand*, Amir R. Masoodi [a] and Niloofar Rajabzadeh-Safaei [b]

Department of Civil Engineering, Ferdowsi University of Mashhad, Iran

(*Received July 12, 2018, Revised January 30, 2019, Accepted march 8, 2019*)

Abstract. This paper is dedicated to nonlinear static and free vibration analysis of Uniform Distributed Carbon Nanotube Reinforced Composite (UD-CNTRC) structures under in-plane loading. The authors have suggested an efficient six-node triangular element. Mixed Interpolation of Tensorial Components (MITC) approach is employed to alleviate the membrane locking phenomena. Moreover, the behavior of the well-known LST element is considerably improved by applying an additional linear interpolation on the strain fields. Based on the rule of mixture, the properties of CNTRC are obtained. In this study, only the uniform distributed CNTs are employed through the thickness direction of element. To achieve the natural frequencies and shape modes, the eigenvalue problem is also solved. Using Total Lagrangian Principles, large amplitude free vibration is considered based on the first normalized mode shape of structure. Different well-known plane problem benchmarks and some proposed ones are studied to validate the accuracy and capability of authors' formulations. In addition, the effects of length to the height ratio of beam, CNT's characteristics, support conditions and normalized amplitude parameter on the linear and nonlinear vibration parameters are investigated.

Keywords: nonlinear vibration; carbon nano-tube; MITC approach; plane triangular element; Total Lagrangian principles

1. Introduction

One of the interesting subjects, which was attracted the attention of researchers, is to investigate the nonlinear static and the dynamic behavior of plane problems, including beams and frames. In this area, developing an efficient element, which can accurately predict the nonlinear behavior of structures, is desired. This kind of formulation leads to the element, which can reach the exact solution by using fewer numbers of elements and reduces the computational costs. Hence, an efficient triangular plane element is formulated for the nonlinear analysis of plane structures. It is obvious that the behavior of plane elements is different from that of beam ones. Based on this fact, an applicable plane element which can analyze beam and frame structures is very useful for researchers. This kind of element can be validated by using well-known beam structures as benchmark and also for the problems having membrane behavior. According to the brief literature review, several researches have concentrated so far on developing new plane elements, which have been employed for the beam and frame structures analyses (Gupta 1979, Allman 1984, Bergan and Felippa 1985, Fajman 2002, Felippa 2003, Liew *et al*. 2006, Tian and Yagawa 2007, Rezaiee-Pajand and Yaghoobi 2014, Rezaiee-Pajand and Rajabzadeh-Safaei 2016, Masoodi and Arabi 2018, Rezaiee-Pajand *et al*. 2018a, d).

Alongside of the element generation, developing new materials and studying their applications in structural engineering attract the attentions of researchers due to high strength and performance with low weight, which are basically suitable for civil and mechanical structures. One of these materials is Carbon Nanotube (CNT). Several researches were performed about investigating the mechanical properties of CNTs Salvetat *et al*. 1999, Allaoui *et al*. 2002, Erik and Chou 2002, Valentini *et al*. 2003, Ansari and Hemmatnezhad 2012, Lin and Xiang 2014a, Heydari *et al*. 2015, Mir *et al*. (2017). Some other peoples investigated the application of CNTs in structures. For instance, single and multi-walled CNTs were studied by Tu and Yang. They explored the influence of the layer number on the effective elastic modulus Tu and Ou-Yang (2002). In 2005, Wan *et al*. used a continuum model to study the mechanisms of load transfer and effective elastic modulus of Single Walled Carbon Nanotube (herein SWCNT). The impacts of CNT length and CNT-matrix inter-phase in (CNTRC) were also considered in that research (Wan *et al*. 2005).

In another paper, bending and local buckling analyses of nano-composite beams reinforced by SWCNT were implemented using the Airy-stress functions by Vodenitcharova and Zhang (2006). Furthermore, Wattanasakulpong and Ungbhakorn decided to present the results of bending, buckling and vibration of CNTRC beams resting on elastic foundation (Wattanasakulpong and Ungbhakorn 2013). In another research, thermal loading was also incorporated in bending, buckling and vibration

*Corresponding author, Ph.D., Professor,
E-mail: rezaiee@um.ac.ir
[a] Ph.D. Candidate, E-mail: amirreza.masoodi@mail.um.ac.ir
[b] Ph.D. Candidate,
E-mail: n.rajabzadehsafaei@mail.um.ac.ir

http://www.techno-press.org/?journal=scs&subpage=6
ISSN: 1229-9367 (Print), 1598-6233 (Online)

analysis of FG-CNTRC beams (Mayandi and Jeyaraj 2015). In 2014, a literature review was provided by Liew *et al*. on the topic of FG-CNTRC structural analysis Liew *et al*. (2015). In a recently published article, a complete analysis was done by Kumar and Srinivas to study the static and dynamic characteristics, including bending, buckling and vibration parameters of FG-CNTRC beams Kumar and Srinivas (2017a). Moreover, an experimental and numerical static bending analysis of CNT reinforced composite plates has been performed by Mehar and Panda (2018). It is obvious that developing formulation to predict the mechanical behavior of FG-CNTRC beams and also other plane problems still attracts the researcher's attentions. On the other hand, other analytical aspects of this topic may be interesting for the investigators.

One of the most important subjects, which have an essential impact on the dynamic behavior of structures, is free vibration analysis specified by obtained linear and nonlinear natural frequencies, based on the geometrically nonlinear analysis. Alijani and Amabili collected a literature review of nonlinear vibration analysis of shells. They discussed on different methods of obtaining nonlinear frequencies of shell structures Alijani and Amabili (2014). According to the authors' knowledge, some new and important works were performed on the linear vibration analysis of beams, especially FG-CNTRC ones. Although several papers were published in the end of 20^{th} century about linear and nonlinear vibration analysis of structures (Mei 1972, 1973, 1986, Rehfield 1973, Gupta 1978, Bhashyam and Prathap 1980, Sarma and Varadan 1982, Iu *et al*. 1985, Dumir and Bhaskar 1988, Sarma *et al*. 1988, Leung and Fung 1989, Singh *et al*. 1990a, b, Weaver Jr. *et al*. 1990, Feng and Bert 1992, Lewandowski 1994, Qaisi 1997, Zhong and Guo 2003, Rezaiee-Pajand and Masoodi 2016, Rezaiee Pajand and Rajabzadeh Safaei 2016b, Sadri *et al*. 2016, Yazdani Sarvestani and Ghayoor 2016, Hirwani *et al*. 2017, Hirwani and Panda 2018, Rezaiee-Pajand *et al*. 2018b), there are not sufficient researches available in which linear and nonlinear vibration of composite beam, especially CNT beam, have been studied in details.

In an interesting paper, Chen *et al*. used incremental harmonic balance method for nonlinear vibration analysis of plane problems. They used beam element in which nonlinear behavior was taken into account by considering longitudinal stretching Chen *et al*. (2001). In 2004, trapezoidal Fourier p-element was employed to investigate the vibration of plane problems by Leung *et al*. They utilized trigonometric functions instead of polynomials to prevent ill-conditioning problem (Leung *et al*. 2004). To obtain free vibration responses of the well-known plane problem, Zhang and Rajendran employed a QUAD4 plane element, which had been developed in the static analysis before Rajendran and Zhang (2007). Based on the finite element formulation, another research was implemented by Yang *et al*. for achieving in-plane vibration. They utilized extended-Hamilton principle to derive the governing differential equation of the curved beams Yang *et al*. (2008). In 2010, the formulations of a multivariable hierarchical beam element were expressed by Yu *et al*. for using in static and vibration analyses. These investigators utilized the generalized variational principle with two kinds of the variables to develop their scheme Yu *et al*. (2010). In one of the newest researches, nonlinear damping effects were studied for obtaining the large-amplitude vibration responses by Amabili. Both numerical and experimental investigations were performed in this research (Amabili 2017). Further, nonlinear vibration of beams composed of viscoelastic materials was performed by Wielentejczyk and Lewandowski. They also examined the stability of steady-state solution Wielentejczyk and Lewandowski (2017). In 2018, Zhou *et al*. could develop a nonlinear quadrature Timoshenko beam element with high accuracy and performance using mechanics-based variables. They employed their proposed element in order to analyze the composite wind turbine blades (Zhou *et al*. 2018). In another research, nonlinear free and forced vibration analysis of curved clamped–clamped beams resting on elastic foundation were numerically implemented using differential integral quadrature method with Newton's iterative solution Mohamed *et al*. (2018).

Recently, Caliò and Greco studied the free vibration responses of the spatial arches. They obtained natural frequencies and mode shapes of Timoshenko beam in which both in-plane and out-of-plane motions were taken into account Caliò and Greco (2014). In 2017, a C^0 enriched quadrilateral element was formulated by Shang *et al*. based on the generalized finite element method. The result was applied for vibration analysis of plane problems considering mesh distortion. In this study, the trigonometric and exponential functions were utilized to enrich the shape functions of the element Shang *et al*. (2017). Alongside of these researches about vibration analysis of beams and plane structures, it was observed that some researchers were attracted into investigating the effects of using composite materials, such as Functionally Graded Mateial (FGM) and Carbon Nanotube (CNT). Although most of these papers were published for the nano-composite beam and plate structures due to more applicability (Zhang *et al*. 2015, Mehar *et al*. 2016, Kumar and Srinivas 2017b, Zhang 2017), few articles have been studied the static and dynamic behaviors of plane structures reinforced by CNT. In 2014, Lin and Xiang implemented the linear free vibration analysis of CNTRC beam. They considered single-walled CNTs for deriving the formulation of their beam element. Accordingly, these investigators incorporated two different types of reinforcement, including Uniform Distributed (UD) and Functionally Graded (FG) CNT reinforcements (Lin and Xiang 2014b). The nonlinear free vibration behavior of functionally graded carbon nanotube reinforced composite flat panel for temperature dependent materials was investigated by Mehar and Panda (2016b). Tahouneh studied the effects of CNTs waviness and aspect ratio on the vibration responses of FG-plate. He considered first and higher-order shear deformation theories of plate. In addition, this investigator implemented linear vibration and mode shape analyses on the sandwich curved panels having MWCNTs FG-reinforcement core in other paper Tahouneh (2017). This study dealt with the modified Halpin-Tsai equation to estimate the effective material properties of FG-MWCNT. Some other researches were concentrated on the bending, buckling and vibration analyses of FG-CNTRC composite plates (Chavan and Lal 2017, Kolahdouzan *et al*. 2018, Tahouneh 2018). In another research, nonlinear vibration analysis of composite laminate beam was done by researchers Shen *et al*. (2017). They considered the effects of thermal environment on the vibration responses of FG graphene-reinforced composite beam. For FG-CNT sandwich structures, an extensive and comprehensive study in the field of linear/nonlinear static and dynamic analyses in thermal environment was presented by Mehar and Panda (Mehar and Panda 2016c, 2018b, c, Mahapatra *et al*. 2017, Mehar *et al*. 2017b, 2018a, b, c). They also studied on the thermomechanical behavior of FG-CNT shear deformable plates (Mehar and Panda 2016a, 2017). Recently, Kumar and Srinivas presented another research, in which complete analyses, including free vibration, bending and buckling of FG-CNTRC beams were performed. They also compared their results with that obtained for hybrid laminated composite beams (Kumar and Srinivas 2017a). Shafiei and Setoodeh performed nonlinear free vibration analysis of FG-CNTRC beams resting on the foundation with nonlinear behavior. They also investigated the post-buckling of this structure Shafiei and Setoodeh (2017). Ding *et al*. could approximately solve the nonlinear transverse vibration of the visco-elastic beam using harmonic balance method. They considered periodic excitation to obtain steady-state responses. Pseudo arc-length method was also employed in their solution procedure Ding *et al*. (2018). In one of the new researches, nonlinear forced vibration of FG-CNTRC curved micro-beam was performed by Allahkarami *et al*. (2018). They used strain gradient theory for deriving the governing equations. Furthermore, Differential Quadrature and Newmark methods were employed to solve the problem.

Based on the stated literature review, there are still interesting topics in this area to be developed by researchers. Accordingly, the main aim of the authors in this paper is to perform the linear and nonlinear vibration analysis of plane structures made of isotropic and UD-CNTs materials by using the high-performance triangular plane element. It is obvious that geometrically nonlinear behaviour of structures is incorporated to obtain nonlinear vibration parameters, including nonlinear natural frequencies and mode shapes. For considering the large deflection of plane structure, Total Lagrangian relation is employed. It should be mentioned that the authors utilize MITC formulation in order to avoid membrane locking phenomena, especially in the nonlinear analysis. On the other hand, an improved procedure is employed to obtain nonlinear natural frequencies and mode shapes based on the obtained first mode shape of structure in the linear analysis as an initial displacement. Hence, the influences of the different ratios of amplitude parameter, CNT's mechanical properties, various support conditions and length to height of beam ratios on the obtained nonlinear responses are studied separately. Findings of several well-known benchmark problems and some suggested novel complicated plane problems indicate the high performance and accuracy of the proposed formulation. Therefore, it can be widely employed in the structures having membrane behaviour, such as, structural shear wall and portal frames.

2. Governing formulations of plane element

In this study, an efficient curved triangular plane element with six nodes, in which there are two transitional degrees of freedom, is considered. The thickness of element is constant and defined by parameter t. It is assumed that this element is made of CNT material. In other words, the geometry of element is similar to Linear Strain Triangular (LST) element. The main contribution of this research is to improve the behavior of this element by using mixed interpolation of strain fields, and make it suitable for complex material. To be more general, the curvilinear coordinate system (r,s) is utilized for this formulation. The thickness of element is assumed to be constant. Accordingly, the geometry field of the element is defined by

$$\mathbf{x} = \sum_{i=1}^{6} N_i(r,s)\mathbf{x}_i \; where \qquad \mathbf{x}_i = \{x_i \quad y_i\}^T \tag{1}$$

where N_i (r, s) is the shape function, which is obtained for iso-parametric six-node triangular element (LST). To obtain the displacement field of the element, the following relation is held

$$\mathbf{u} = \sum_{i=1}^{6} N_i(r,s)\mathbf{u}_i \; where \qquad \mathbf{u}_i = \{u_i \quad v_i\}^T \tag{2}$$

Here, the horizontal and vertical displacements are defined by u_i and v_i, respectively. The covariant strain tensor, including the linear and nonlinear parts, is written in the following form

$$\begin{aligned} {}_0^t\boldsymbol{\varepsilon}_{ij} &= {}_0^t\mathbf{e}_{ij} + {}_0^t\boldsymbol{\eta}_{ij} \\ {}_0^t\mathbf{e}_{ij} &= \frac{1}{2}\left({}_0^t\mathbf{g}_i \cdot {}_0^t\mathbf{u}_{,j} + {}_0^t\mathbf{g}_j \cdot {}_0^t\mathbf{u}_{,i} \right) \\ {}_0^t\boldsymbol{\eta}_{ij} &= \frac{1}{2}\, {}_0^t\mathbf{u}_{,i} \cdot {}_0^t\mathbf{u}_{,j} \end{aligned} \tag{3}$$

where, $\mathbf{e}_{ij}$ and $\boldsymbol{\eta}_{ij}$ are the linear and nonlinear Green-Lagrange strain tensors. Moreover, the covariant base vector and first derivation of the displacements relative to the local convected coordinates vectors are defined by $\mathbf{g}_i$ and $\mathbf{u}_{,i}$, as follows

$$\mathbf{g}_i = \frac{\partial \mathbf{x}}{\partial r_i}, \quad \mathbf{u}_{,i} = \frac{\partial \mathbf{u}}{\partial r_i} \quad : \qquad r_1 = r \quad \text{and} \quad r_2 = s \tag{4}$$

To consider the geometric nonlinear behavior, Total Lagrangian principles are utilized. In the common way, the strain vector is presented in the below form

$$\boldsymbol{\varepsilon}_{ij} = \{\varepsilon_{11} \quad \varepsilon_{22} \quad 2\varepsilon_{12}\}^T \tag{5}$$

Note that, $\varepsilon_{11} = \varepsilon_{rr}$, $\varepsilon_{22} = \varepsilon_{ss}$ and $\varepsilon_{33} = \varepsilon_{rs}$. To improve the behavior of element and alleviate the membrane locking, a mixed interpolation is applied to the local strains using the tying points. The assumed covariant strain components are defined using the following relation

$$\tilde{\varepsilon}_{ij}(r,s)=\sum_{k=1}^{m_{ij}} N_{ij}(r,s)\varepsilon_{ij}\Big|_{(r_{ij}^{k},s_{ij}^{k})} \tag{6}$$

where m_{ij} is the number of tying points. The interpolation of strains starts using the linear interpolation functions as follows

$$\begin{aligned}\tilde{\varepsilon}_{rr} &= a_1+b_1 r+c_1 s\\ \tilde{\varepsilon}_{ss} &= a_2+b_2 r+c_2 s\\ \tilde{\varepsilon}_{nn} &= a_3+b_3 r+c_3(1-r-s)\end{aligned} \tag{7}$$

In which, $\tilde{\varepsilon}_{nn}$ is the normal strain of the oblique side of triangular stress element. To achieve the nine unknown constants of Eq. (7), one can find $\tilde{\varepsilon}_{rs}$ in the terms of $\tilde{\varepsilon}_{rr}$, $\tilde{\varepsilon}_{ss}$ and $\tilde{\varepsilon}_{nn}$

$$\tilde{\varepsilon}_{rs}=0.5(\tilde{\varepsilon}_{rr}+\tilde{\varepsilon}_{ss})-\tilde{\varepsilon}_{nn} \tag{8}$$

The linear interpolations between nine tying points are shown in Fig. 1. In addition, Table 1 presents the position of tying points in the local system.

Applying the conditions of satisfying the strains at tying points, gives the values of unknown constants

$$\begin{aligned}&\tilde{\varepsilon}_{rr}(0,0)=m\varepsilon_{1rr}^{(1)}+l\varepsilon_{2rr}^{(1)},\quad \tilde{\varepsilon}_{rr}(1,0)=l\varepsilon_{1rr}^{(1)}+m\varepsilon_{2rr}^{(1)}\\ &\tilde{\varepsilon}_{rr}(1/2,0)=\frac{1}{2}(m+l)(\varepsilon_{1rr}^{(1)}+\varepsilon_{2rr}^{(1)}),\quad \tilde{\varepsilon}_{rr}(1/2-1/2\sqrt{3},1/\sqrt{3})=\varepsilon_{crr}^{(1)}\\ &\tilde{\varepsilon}_{ss}(0,0)=m\varepsilon_{1ss}^{(2)}+l\varepsilon_{2ss}^{(2)},\quad \tilde{\varepsilon}_{ss}(0,1)=l\varepsilon_{1ss}^{(2)}+m\varepsilon_{2ss}^{(2)}\\ &\tilde{\varepsilon}_{ss}(0,1/2)=\frac{1}{2}(m+l)(\varepsilon_{1ss}^{(2)}+\varepsilon_{2ss}^{(2)}),\quad \tilde{\varepsilon}_{ss}(1/\sqrt{3},1/2-1/2\sqrt{3})=\varepsilon_{css}^{(2)}\\ &\tilde{\varepsilon}_{nn}(1,0)=m\varepsilon_{1nn}^{(3)}+l\varepsilon_{2nn}^{(3)},\quad \tilde{\varepsilon}_{nn}(0,1)=l\varepsilon_{1nn}^{(3)}+m\varepsilon_{2nn}^{(3)}\\ &\tilde{\varepsilon}_{nn}(1/2,1/2)=\frac{1}{2}(m+l)(\varepsilon_{1nn}^{(3)}+\varepsilon_{2nn}^{(3)}),\quad \tilde{\varepsilon}_{nn}(1/2-1/2\sqrt{3},1/2-1/2\sqrt{3})=\varepsilon_{cnn}^{(3)}\\ &m=\frac{1}{2}(1+\sqrt{3}),\quad l=\frac{1}{2}(1-\sqrt{3})\end{aligned} \tag{9}$$

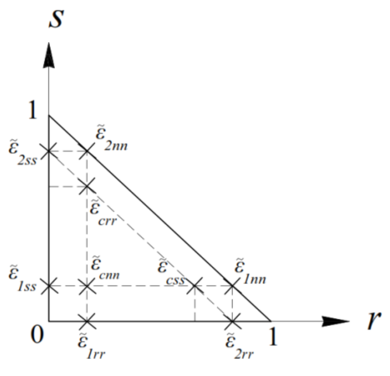

Fig. 1 The schematic position of tying points for strain interpolation

Table 1 The tying points positions

$\boldsymbol{\varepsilon}$	$\boldsymbol{r}$	$\boldsymbol{s}$
$\tilde{\varepsilon}_{1rr}$	$\frac{1}{2}-\frac{1}{2\sqrt{3}}$	0
$\tilde{\varepsilon}_{1ss}$	0	$\frac{1}{2}-\frac{1}{2\sqrt{3}}$
$\tilde{\varepsilon}_{cnn}$	$\frac{1}{2}-\frac{1}{2\sqrt{3}}$	$\frac{1}{2}-\frac{1}{2\sqrt{3}}$
$\tilde{\varepsilon}_{2rr}$	$\frac{1}{2}+\frac{1}{2\sqrt{3}}$	0
$\tilde{\varepsilon}_{2ss}$	0	$\frac{1}{2}+\frac{1}{2\sqrt{3}}$
$\tilde{\varepsilon}_{2nn}$	$\frac{1}{2}-\frac{1}{2\sqrt{3}}$	$\frac{1}{2}+\frac{1}{2\sqrt{3}}$
$\tilde{\varepsilon}_{1nn}$	$\frac{1}{2}+\frac{1}{2\sqrt{3}}$	$\frac{1}{2}-\frac{1}{2\sqrt{3}}$
$\tilde{\varepsilon}_{crr}$	$\frac{1}{2}-\frac{1}{2\sqrt{3}}$	$\frac{1}{\sqrt{3}}$
$\tilde{\varepsilon}_{css}$	$\frac{1}{\sqrt{3}}$	$\frac{1}{2}-\frac{1}{2\sqrt{3}}$

To transform the Green-Lagrange strain from the local curvilinear coordinate system to global Cartesian system, contravariant base vectors are employed, as follows

$$\underline{\hat{\boldsymbol{\varepsilon}}}=\boldsymbol{\varepsilon}_{ij}\,\mathbf{g}^{i}\,\mathbf{g}^{j} \tag{10}$$

in which $\mathbf{g}^{i}$ is contravariant base vector, which can be calculated by using the next metric vector and covariant components of metric tensor g^{ij}

$$\mathbf{g}^{i}=g^{ij}\,\mathbf{g}_{j} \tag{11}$$

The tensorial form of the second Piola-Kirchhoff stress can be achieved by utilizing the following relation

$$\mathbf{S}^{ij}=\mathbf{C}^{ijkl}\,\underline{\hat{\boldsymbol{\varepsilon}}}_{kl} \tag{12}$$

where $\mathbf{C}^{ijkl}$ is the fourth-order tensor of material, which is obtained in the convected coordinates. To establish the finite element stiffness matrix, the following linearized governing relations for two states of the linear and nonlinear analyses are available based on the principle of virtual work

$$\begin{aligned}\int_{{}^{0}V}{}_{0}\mathbf{S}^{ij}.\delta_{0}\hat{\mathbf{\varepsilon}}_{ij}\,d\,{}^{0}V+\int_{{}^{0}V}{}_{0}^{t}\mathbf{S}^{ij}.\delta_{0}\hat{\boldsymbol{\eta}}_{ij}\,d\,{}^{0}V\\ ={}^{t+\Delta t}\mathbf{R}-\int_{{}^{0}V}{}_{0}^{t}\mathbf{S}^{ij}.\delta_{0}\hat{\mathbf{e}}_{ij}\,d\,{}^{0}V\end{aligned} \tag{13}$$

in which $\mathbf{R}$ is the external virtual work. It is worth mentioning that using 3 Guass points for numerically integration of the first and second parts of the left side of Eq. (12), the linear and nonlinear parts of stiffness matrices are calculated.

3. Linear and nonlinear vibration solution

If the structural system behaves nonlinearly, the linear frequency domain analysis will not be desirable to reflect all nonlinear characteristics. To overcome this limitation, nonlinear frequency responses can be utilized to consider nonlinear dynamic effects. The nonlinear frequency response can reveal complex resonance, which cannot be seen in linear state Billings (2013). In this section, the authors present the procedure used for obtaining the linear and nonlinear vibration analysis of the plane structures. By substituting the kinetic energy relation into linearized governing Eq. (12), the following equality is obtained

$$\begin{aligned}&\int_{{}^{0}V} {}_{0}^{t}\ddot{\mathbf{u}}_i \, {}^{0}\rho \delta \, {}_{0}^{t}\mathbf{u}_i \, d\,{}^{0}V + \int_{{}^{0}V} {}_{0}\mathbf{S}^{ij} \, \delta \, {}_{0}\hat{\boldsymbol{\varepsilon}}_{ij} \, d\,{}^{0}V \\ &+ \int_{{}^{0}V} {}_{0}^{t}\mathbf{S}^{ij} \, \delta \, {}_{0}\hat{\boldsymbol{\eta}}_{ij} \, d\,{}^{0}V = {}^{t+\Delta t}\mathbf{R} - \int_{{}^{0}V} {}_{0}^{t}\mathbf{S}^{ij} \, \delta \, {}_{0}\hat{\mathbf{e}}_{ij} \, d\,{}^{0}V\end{aligned} \tag{14}$$

To achieve the vibration responses, including natural frequencies and mode shapes, the subsequent eigenvalue problem should be solved

$$\left|\mathbf{K} - \omega^2 \mathbf{M}\right| = 0 \tag{15}$$

in which **K** and **M** are the stiffness and mass matrices, respectively. In order to derive the mass matrix, the following relation is employed

$$\mathbf{M} = \int_{{}^{0}V} N_i^T \, {}^{0}\rho N_i \, d\,{}^{0}V \tag{16}$$

where N_i is the shape function of node i. In addition, ρ is mass density. It is proven that FEM is a reliable technique to use in the vibration analysis of complicated structures. It is obvious that for the linear vibration analysis, the linear part of the stiffness matrix is used, while to obtain the nonlinear natural frequencies, the nonlinear part of the stiffness matrix should be added to the linear one ($\mathbf{K} = \mathbf{K}_L + \mathbf{K}_{NL}$). For performing nonlinear vibration analysis, the first normalized mode shape vector is applied to the structure as an initial deflection. Different ratios of the amplitude vibration parameter (a/r) are considered for the nonlinear vibration analysis. An iterative solution method, such as Newton-Raphson scheme, is employed for performing structural nonlinear analysis. In fact, Eq. (14) is solved numerically based on the following procedure:

Step 1: Evaluating the global stiffness and mass matrices using the proposed FEM and assembly process.

Step 2: Linear eigenvalue problem of Eq. (14) ($|\mathbf{K}_L - \omega^2\mathbf{M}| = 0$) should be solved to obtain the linear natural frequencies and mode shapes.

Step 3: Extract the first mode eigenvector. This should be normalized by using the amplitude vibration ratio. In order to obtain the modified nonlinear stiffness matrix, the first mode's eigenvector is used to modify the nodal positions.

Step 4: The nonlinear eigenvalue problem of Eq. (14) ($|\mathbf{K}_L + \mathbf{K}_{NL} - \omega^2\mathbf{M}| = 0$) is solved iteratively by using Newton-Raphson solution method. The following relations are considered as the convergence criterion

$$\begin{aligned}&\left|\omega_{i^{th}} - \omega_{i+1^{th}}\right| \le Tolerance \\ or \quad & \\ &\left\|{}^{1}V_{i^{th}} - {}^{1}V_{i+1^{th}}\right\| \le Tolerance\end{aligned} \tag{17}$$

where, V is the vector of mode shape values, which is normalized in each iteration. It is obvious that a known tolerance for the numerical convergence should be specified. If the convergence criterion is not satisfied, the procedure is repeated from Step 2. Otherwise, the fundamental nonlinear frequencies are obtained and the ratio of nonlinear frequency to the linear one is also calculated.

4. Carbon Nanotube Reinforced Composites (CNTRC)

In this section, the authors express the corresponded formulations, which are employed for incorporating the effects of CNTs on the mechanical behavior of structures. To reach this purpose, the governing constitutive matrix of the plane element should be changed. It is important to state that these materials are used due to their high strength and low weight. The CNTRC layer includes an isotropic polymer matrix and multi-walled CNTs (hereafter MWCNT). It is assumed that the effect of the interface is ignored. It should be mentioned that due to complexity of MWCNT formulations, an effective elastic characteristic can be employed. Hence, an equality, which was proposed by Tu and Ou-Yang, is defined as follows (Tu and Ou-Yang 2002, Rezaiee Pajand *et al*. 2018e, 2019)

$$X_i^{mw} = \frac{N_w t_{cnt} X_i^{sw}}{(N_w - 1)h_{in} + t_{cnt}} \tag{18}$$

In the last relation, X_i^{mw} and X_i^{sw} are the corresponded elastic characteristics of MWCNTs and SWCNTs, respectively. Moreover, the thickness of walls and inter wall spacing are defined by t_{cnt} and h_{in}. It should be added that N_w is used to indicate the number of walls used in CNTRC layer. Note that the elastic properties of MWCNTs and SWCNTs are the same if the value of N_w is equal to 1. For CNTRC solid structure problem, the dependent mechanical and physical properties are elastic modulus (E), Poisson's ratio (ν) and mass density (ρ). A simple solid structure problem, which is investigated in this case, is a beam. To the best knowledge of the authors and the complete literature review, there are little studies about this topic. However, the nonlinear bending and vibration analysis of beam structure can still attract the attention of researchers. Thus, the authors decide to investigate the nonlinear behavior of SW-CNTRC beam using the proposed triangular plane element and Green-Lagrange strain formulations.

There are many techniques to estimate the mechanical properties of CNT reinforced composites such as Mori-Tanaka, rule of mixture, Halpin-Tsai, etc. Among those, rule of mixture is one of the first schemes that has been used extensively due to the simplicity and convenience. Moreover, this method is suitable for unidirectional composites. On the other hand, Mori-Tanaka scheme is applicable for either unidirectional or randomly oriented CNT reinforced composites. However, for unidirectional cases these two techniques are almost equal (Mehar *et al*. 2017a). Therefore, to find the mechanical and physical properties, the next rule of mixture is utilized (Shen 2009)

$$V_m + V_{cnt} = 1 \tag{19}$$

in which V_m and V_{cnt} indicate the volume fraction of polymer matrix and CNT fibers, respectively. Based on the Eq. (18), the following equalities can be employed for the elastic properties of the CNTRC beam by considering the orthotropic behavior of SWCNT

$$\begin{aligned} E_{11} &= \beta_1 V_{cnt} E_{11}^{cnt} + V_m E^m \\ \frac{\beta_2}{E_{22}} &= \frac{V_{cnt}}{E_{22}^{cnt}} + \frac{V_m}{E^m} \\ \frac{\beta_3}{G_{12}} &= \frac{V_{cnt}}{G_{12}^{cnt}} + \frac{V_m}{G^m} \end{aligned} \tag{20}$$

in which G is the shear modulus. The constant coefficients of CNT efficiency are defined by β_i for i = 1, 2, 3 that were calculated according to the nano-scale size effect. Table 2 presents the values of this factor for different amounts of CNTs volume fraction. In addition, the Poisson's ratios have the succeeding relations

$$\nu_{12} = V_{cnt}\nu_{12}^{cnt} + V_m \nu^m \qquad \nu_{21} = \frac{E_{22}}{E_{11}}\nu_{12} \tag{21}$$

The mass density is presented in the following form

$$\rho = V_{cnt}\rho_{12}^{cnt} + V_m \rho^m \tag{22}$$

In this study, the distribution of the CNTs (UD-CNT) is assumed to be uniform along the thickness direction of structure. Accordingly, the volume fraction of CNT in the terms of the CNTs mass fraction and density of the constituent is calculated by

$$V_{cnt} = \frac{w_{cnt}}{\left[1 - \left(\frac{\rho^{cnt}}{\rho^m}\right)\right] w_{cnt} + \left(\frac{\rho^{cnt}}{\rho^m}\right)} \tag{23}$$

where, w_{cnt} is mass fraction. The constitutive stress-strain matrix can be derived in the below form

$$\mathbf{C}^{ijkl} = \begin{bmatrix} C^{1111} & C^{1122} & 0 \\ C^{1122} & C^{2222} & 0 \\ 0 & 0 & C^{1212} \end{bmatrix} \tag{24}$$

Table 2 The efficiency coefficients of CNTs

Coefficient (β_i)	V_{cnt}		
	0.12	0.17	0.28
β_1	1.2833	1.3414	1.3238
β_2	1.0556	1.7107	1.7380
β_3	1.0556	1.7107	1.7380

in which the components of $\mathbf{C}^{ijkl}$ are defined as follows

$$\begin{aligned} &C^{1111} = \frac{E_{11}}{\Delta} \qquad && C^{2222} = \frac{E_{22}}{\Delta} \\ &C^{1122} = \frac{E_{11}\nu_{21}}{\Delta} \qquad && C^{1212} = G_{12} \\ &\Delta = 1 - \nu_{12}\nu_{21} \end{aligned} \tag{25}$$

5. Numerical examples

This part deals with the application of the employed plane element in the linear and nonlinear free vibration analysis. During the linear vibration analysis, only the linear part of the stiffness matrix is considered. In addition, a simple Newton-Raphson iterative solution is utilized to reach the nonlinear vibration parameters by employing the geometric nonlinear stiffness matrix. Three-Gauss points are used in order to accomplish numerical integration. In addition, the rate of convergence is checked for the case of homogenous plane problems. Different boundary conditions are also considered for the selected examples. On the other hand, the authors implement the linear and nonlinear vibration analysis of the plane structures by solving an eigenvalue problem to obtain the vibration parameters, especially the natural frequencies and mode shapes. First, a convergence study is performed to obtain the optimum and required number of elements. Then, the authors implement the nonlinear analysis using the optimum mesh discretization. Various values of the vibration amplitude ratio are considered for the nonlinear vibration analysis. It is worth mentioning that the initial deformation, which should be applied to the structure, is calculated based on the first normalized mode shape.

5.1 Straight beam with different boundary conditions

The first problem which can be solved to validate the proposed formulation is the linear and nonlinear vibration analysis of a straight beam. This structure is modeled using different numbers of elements. Accordingly, the results can present a convergence study, and lead to an optimum state of the mesh discretization for the nonlinear vibration analysis. After performing this action, the obtained optimum number of elements is found to be equal to 64. To present the comprehensive solutions for the natural frequencies and mode shapes, different support conditions, including Hinged-Hinged (H-H) and Clamped-Clamped (C-C) are applied. For the (H-H) and (C-C) conditions, the authors take benefit of the structural symmetry, and half of the beam is modeled. Fig. 2 demonstrates the mesh

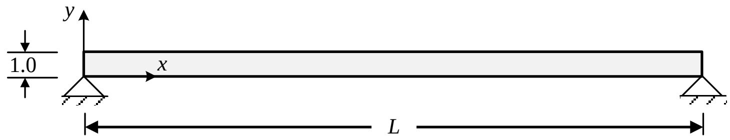

(a) Hinged-hinged

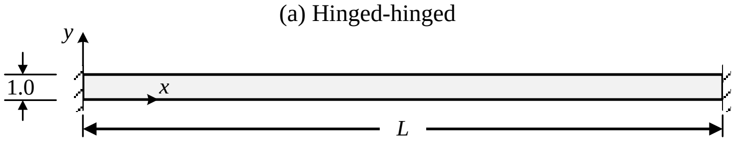

(b) Clamped-clamped

(c) 24 elements

(d) 32 elements

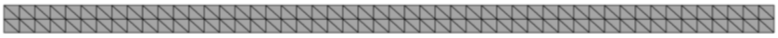

(e) 200 elements

Fig. 2 The geometry and mesh discretization of straight beam

discretization used for this structure.

It is clear that the slenderness ratio of the beam is effective on the vibration responses. To investigate this subject, various ratios for slenderness parameter, L/r, are utilized. The character r refers to the radius of gyration, while L is the length of the beam. In this problem, the elastic modulus and Poisson's ratio are equal to *1* and *zero*, respectively. Moreover, the density parameter is assumed to be *1*. A convergence study is performed to find the optimum number of elements for mesh discretization. The results are provided for two cases of support conditions, including H-H and C-C in Table 3 and Figs. 3(a) and (b), respectively.

To investigate the effects of the slenderness ratio on the vibration responses, different values of L/r, including, 50, 100 and 150 are considered. In the case of $L/r = 100$ and 150, the beam is assumed to be very thin. Consequently, this validation can show the high performance of proposed element for alleviating the locking phenomena occurring especially in thin structures. To reach this conclusion, the following geometry properties for the beam are used

$$b = 1.0 \qquad t = 1.0 \qquad r = \frac{1}{\sqrt{12}}$$

Table 3 First four natural frequencies of the straight beam

	H-H (L/r = 100)				C-C (L/r = 100)			
ω_L^i	i = 1	i = 2	i = 3	i = 4	i = 1	i = 2	i = 3	i = 4
Present (64 elements)	0.0034	0.0136	0.0305	0.0539	0.0077	0.0212	0.0414	0.0679
Rao (2007)	0.0034	0.0136	0.0307	0.0547	0.0077	0.0213	0.0419	0.0692

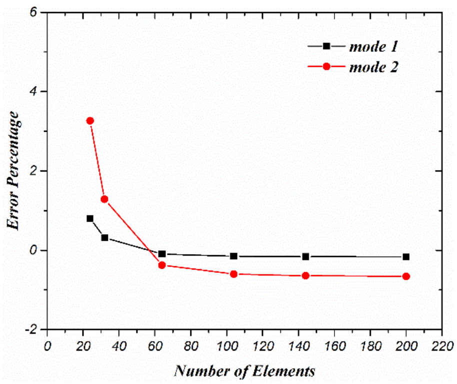

(a) H-H supports

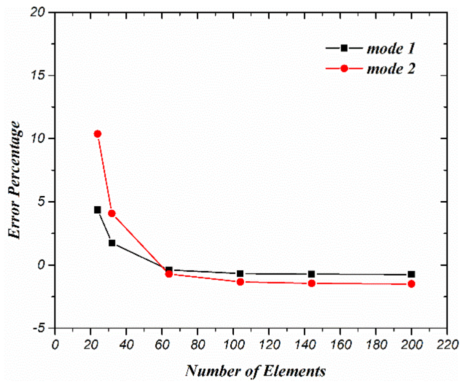

(b) C-C supports

Fig. 3 Convergence study of linear vibration analysis of the straight beam

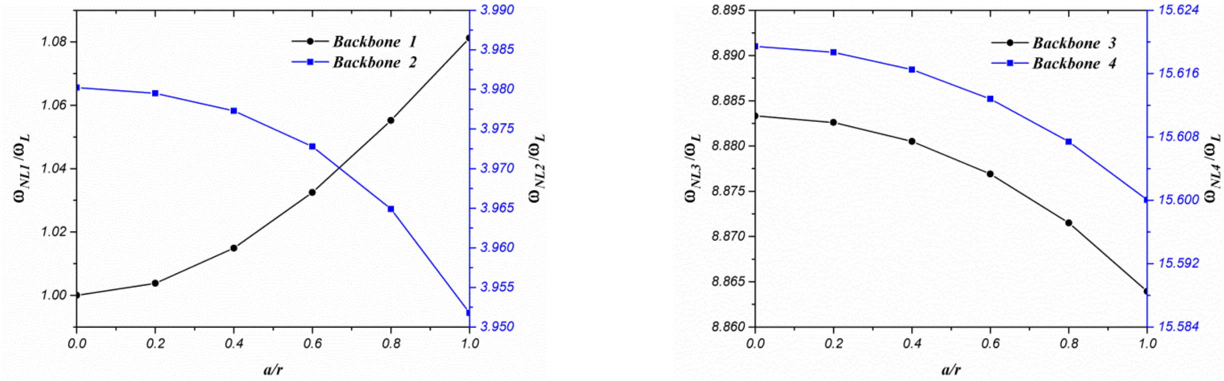

(a) First and second modes (b) Third and fourth modes

Fig. 4 Backbone curves of the H-H thin beam

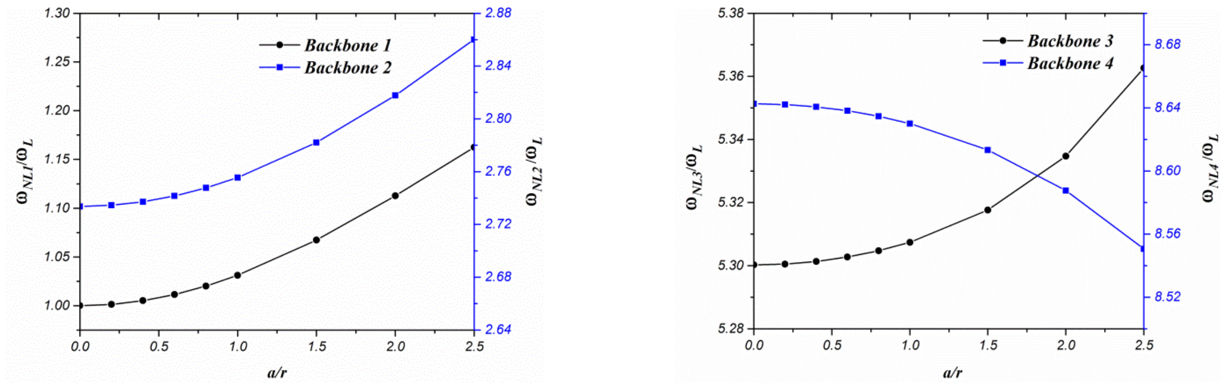

(a) First and second modes (b) Third and fourth modes

Fig. 5 The backbone curves of the C-C thin beam

Table 4 Nonlinear vibrations of the straight beam

BCs	$\frac{a}{r}$	$\frac{\omega_{NL}^i}{\omega_L^i}$				
		i = 1		i = 2	i = 3	i = 4
		Present	Bhashyam and Prathap (1980), Marur and Prathap (2005), Rao (2007)			
H-H (L/r = 100)	0.0	1.0000	**1.0000**	3.9802	8.8833	15.6194
	0.2	1.0038	**1.0037**	3.9795	8.8826	15.6187
	0.4	1.0149	**1.0149**	3.9773	8.8805	15.6165
	0.6	1.0325	**1.0331**	3.9728	8.8769	15.6128
	0.8	1.0552	**1.0580**	3.9649	8.8715	15.6074
	1.0	1.0812	**1.0892**	3.9518	8.8639	15.6001
C-C (L/r = 100)	0.0	1.0000	**1.0000**	2.7336	5.3003	8.6426
	0.2	1.0013	**1.0012**	2.7346	5.3005	8.6421
	0.4	1.0051	**1.0048**	2.7372	5.3013	8.6406
	0.6	1.0114	**1.0110**	2.7416	5.3027	8.6382
	0.8	1.0201	**1.0189**	2.7477	5.3047	8.6347
	1.0	1.0311	**1.0295**	2.7555	5.3074	8.6301
	1.5	1.0672	**1.0650**	2.7821	5.3176	8.6133
	2.0	1.1127	**1.1127**	2.8177	5.3347	8.5876
	2.5	1.1624	----	2.8601	5.3626	8.5506

In the line of responses' validation, different pervious solutions can be employed (Rao and Raju 2003, Marur and Prathap 2005). The linear and nonlinear responses for C-C and H-H support conditions are compared with the available results. To obtain the ratio of the nonlinear natural frequencies to the first linear one, several ratios of large amplitude, including 0.2, 0.4, 0.6, 0.8, 1.0, 1.5 and 2.0 are considered. After that, the results are provided for the different ratios of $\omega_{NL}^{i}/\omega_{L}^{1}$, in which superscript i defines the number of modes. For the slenderness ratio of 100, the corresponded backbone curves are provided in Fig. 4 for H-H supports. It is observed that for the first mode, the ratio of the first nonlinear natural frequency to first linear one increases by enhancing the ratio of amplitude vibration while this ratio for other modes decreases. Fig. 5 shows the related curves for C-C support condition. For this case, all ratios of the nonlinear natural frequencies to linear one increase except the fourth mode. Table 4 reports the ratios of the nonlinear natural frequencies to the linear one for some values of the amplitude vibration parameter.

In this investigation, the effect of the slenderness ratio on the backbone curves for the straight beam is studied. The related backbone curves of the first two modes are provided for different ratios of slenderness, including, 50, 100 and 150. Plots in Figs. 6-7 illustrate these curves for H-H and C-C support conditions, respectively.

It is observed that the effect of the slenderness ratio on the nonlinear vibration responses of H-H beam is more than C-C beam. For the slenderness ratios in the range of 50 to 150, this effect can be ignored in the C-C beam and for the first mode. On the other hand, the effects of support conditions on the nonlinear vibration responses are investigated. Consequently, the backbone curves are also provided for the first four modes of the thin beam with the slenderness ratio of 100 for two cases of support conditions in Fig. 8. The shapes of the first four modes are depicted for two states of H-H and C-C straight beam in Figs. 9-10, respectively. To show the mode shapes of the beam smoothly and clearly, 200 triangular elements are employed.

5.2 In-plane vibration of cantilever square plate

A cantilever square plane problem, shown in Fig. 11(a), is analyzed. The structural dimensions and mesh refinement are depicted in Figs. 11(b)-(d). The value of thickness is equal to 1.0. For this plane stress state, the material parameters E = 1.0, ν = 0.3 and ρ = 1.0 are considered.

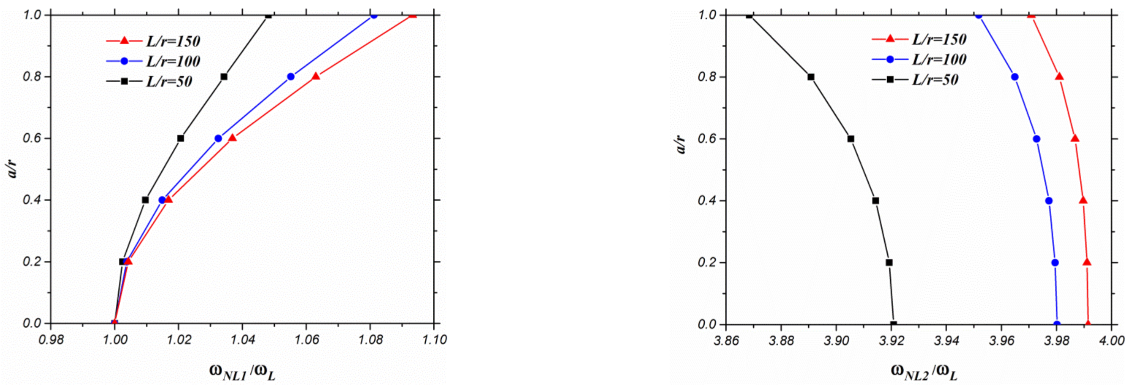

(a) Mode 1 (b) Mode 2

Fig. 6 The effect of slenderness ratio on the backbone curves for H-H beam

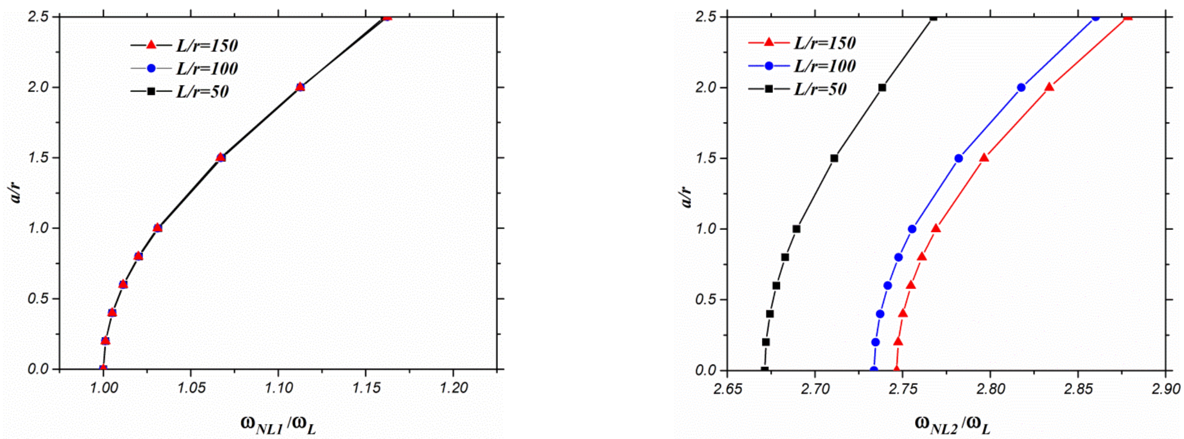

(a) Mode 1 (b) Mode 2

Fig. 7 The effect of slenderness ratio on the backbone curves for C-C beam

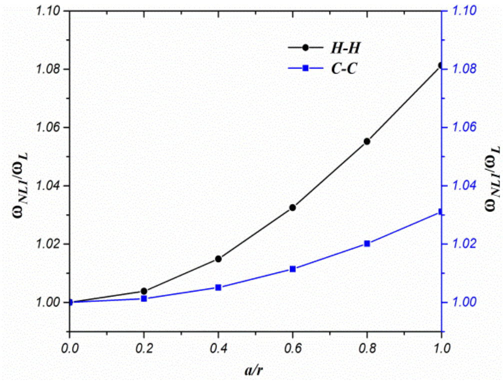

(a) Mode 1

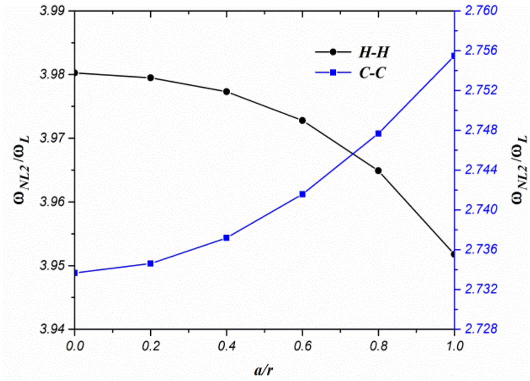

(b) Mode 2

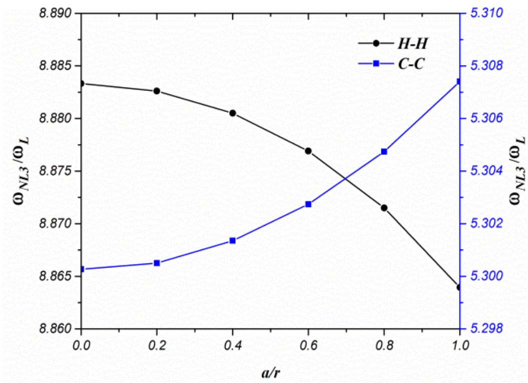

(c) Mode 3

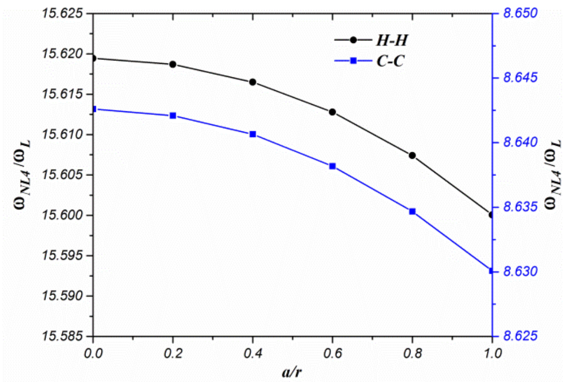

(d) Mode 4

Fig. 8 The effect of support conditions on the nonlinear vibration responses

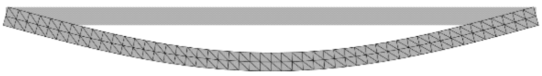

(a) Mode 1

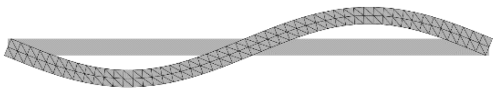

(b) Mode 2

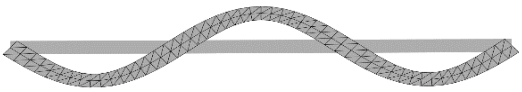

(c) Mode 3

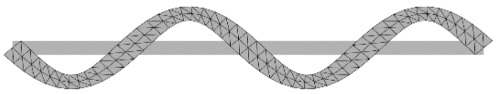

(d) Mode 4

Fig. 9 Different mode shapes of H-H straight beam

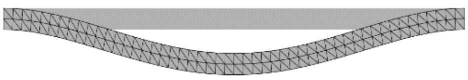

(a) Mode 1

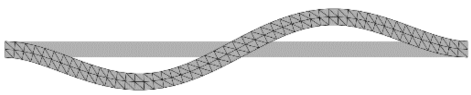

(b) Mode 2

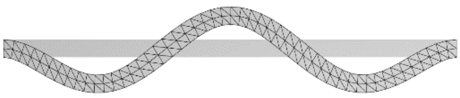

(c) Mode 3

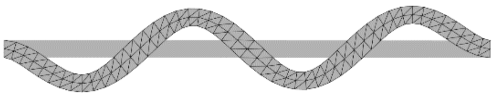

(d) Mode 4

Fig. 10 Different mode shapes of C-C straight beam

The in-plane vibration of this problem was also investigated by Gupta using 20×20 mesh, involving higher-order dynamic correction terms related to stiffness and mass matrices (Gupta 1978). Other researchers have solved this problem to obtain the linear solution for the natural frequencies (Leung *et al*. 2004, Shang *et al*. 2017). At this

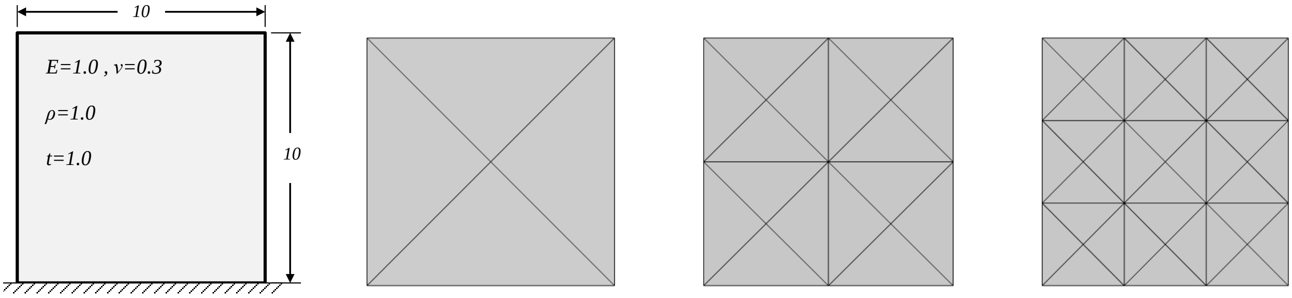

(a) Square plate (b) 4 elements (c) 16 elements (d) 36 elements

Fig. 11 The geometry and mesh discretizations of cantilever square plate

stage, a convergence study for obtaining an optimum mesh discretization is performed, whose curves for the different number of the proposed triangular elements is shown in Fig. 12. Afterwards, the results are employed for the nonlinear vibration analysis. In addition, the linear responses of natural frequencies are reported in Table 5. Moreover, the obtained mode shapes of the cantilever square plate discritized by 36 elements are depicted in Fig. 13.

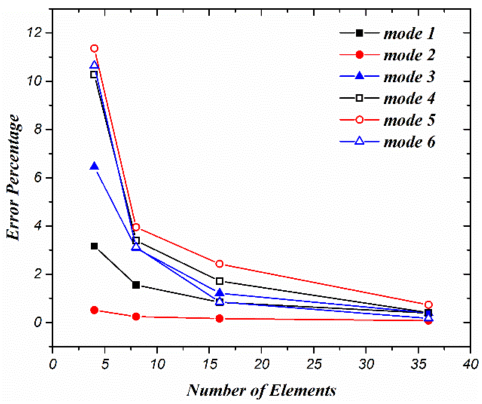

Fig. 12 Convergence study of six linear natural frequencies for the cantilever square plate

On the other hand, the nonlinear responses of natural frequencies are provided based on different values of the amplitude vibration ratio. These results are presented in Table 6. Moreover, the corresponded backbone curves are provided in Fig. 14.

5.3 In-plane vibration of a trapezoid dam

In this section, a trapezoid dam is considered, whose structural geometry and mesh is depicted in Fig. 15. This

Table 6 Nonlinear vibrations of the cantilever square plate

$\frac{a}{r}$	$\frac{\omega_{NL}^i}{\omega_L^i}$			
	$i = 1$	$i = 2$	$i = 3$	$i = 4$
0	1.00000	2.39362	2.69307	4.28011
0.1	0.99702	2.39259	2.68887	4.27438
0.2	0.98806	2.38952	2.67628	4.25716
0.3	0.97282	2.38434	2.65495	4.22766
0.4	0.95046	2.37686	2.62389	4.18398
0.5	0.91933	2.36664	2.58104	4.12209
0.6	0.87568	2.35236	2.52123	4.03164

Table 5 Linear natural frequencies of the cantilever square plate

ω_L^i	$i = 1$	$i = 2$	$i = 3$	$i = 4$	$i = 5$	$i = 6$
Present	0.0660	0.1581	0.1778	0.2827	0.3059	0.3228
Shang *et al.* (2017)	**0.0658**	**0.1580**	**0.1772**	**0.2816**	**0.3037**	**0.3223**
Leung and Fung (1989)	**0.0660**	**0.1580**	**0.1775**	**0.2819**	**0.3044**	**0.3225**

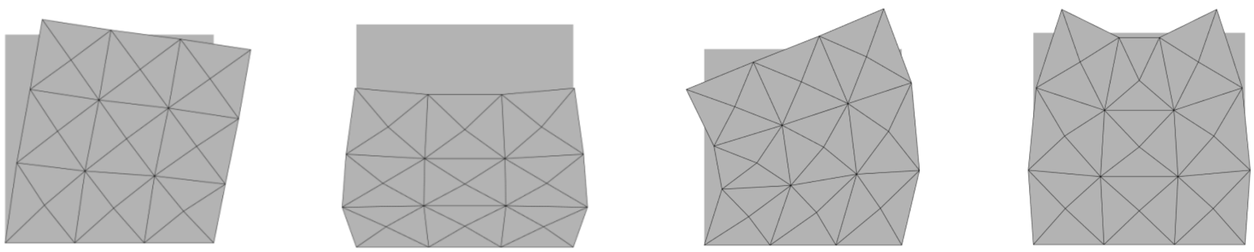

(a) Mode 1 (b) Mode 2 (c) Mode 3 (d) Mode 4

Fig. 13 The first four mode shapes of cantilever square plate

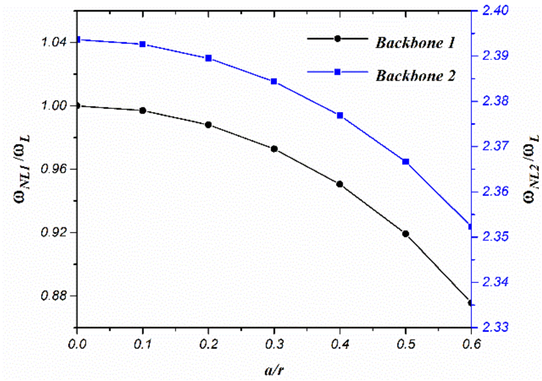

(a) First and second modes

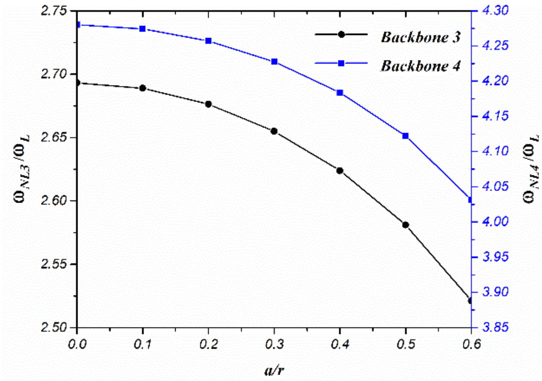

(b) Third and fourth modes

Fig. 14 The backbone curves of the cantilever square plate

problem was also solved in other studies such as Leung *et al*. (Leung *et al*. 2004, Shang *et al*. 2017). The mechanical and physical parameters are: E = 1.0, ν = 0.3 and ρ = 1.0. For this structure, the authors implement a convergence study for the first eight natural frequencies to reach the optimum number and type of mesh discretization. After

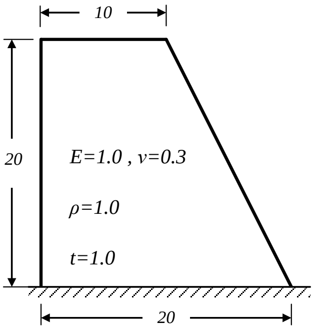

(a) Schematic

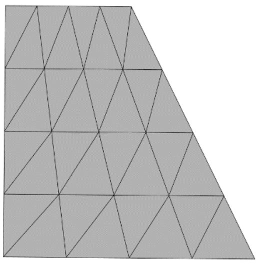

(b) Mesh discretization

Fig. 15 Trapezoid dam

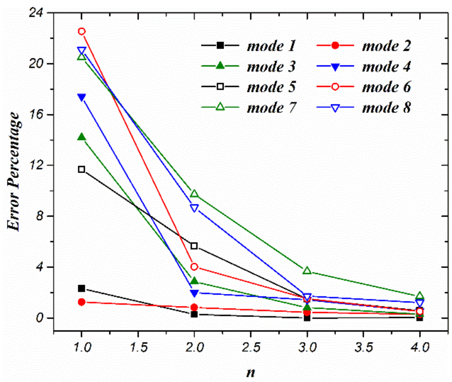

Fig. 16 Convergence study of the eight linear natural frequencies for the trapezoid dam

Table 7 Nonlinear and linear vibrations of the trapezoid dam

$\frac{a}{r}$	$\frac{\omega_{NL}^i}{\omega_L^i}$			
	i = 1	i = 2	i = 3	i = 4
0	1.00000	2.30520	2.62819	4.73129
0.1	0.99838	2.30112	2.63036	4.73185
0.2	0.99504	2.29612	2.62974	4.72948
0.3	0.98982	2.29003	2.62620	4.72401
0.4	0.98251	2.28263	2.61955	4.71512
0.5	0.97278	2.27354	2.60949	4.70230
0.6	0.96014	2.26223	2.59559	4.68476
0.7	0.94373	2.24774	2.57716	4.66106
0.8	0.92192	2.22815	2.55295	4.62839

	ω_L^i			
Present	0.0373	0.0859	0.0979	0.1764
Shang *et al*. (2017)	**0.0373**	**0.0862**	**0.0977**	**0.1755**
Leung and Fung (1989)	**0.0374**	**0.0863**	**0.0983**	**0.1767**

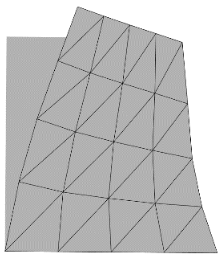

(a) Mode 1

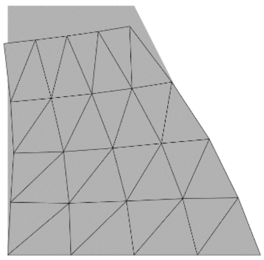

(b) Mode 2

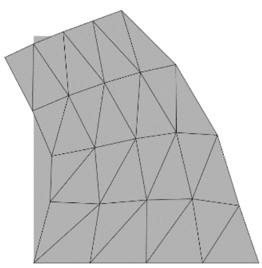

(c) Mode 3

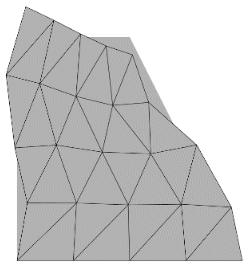

(d) Mode 4

Fig. 17 The mode shapes of trapezoid dam

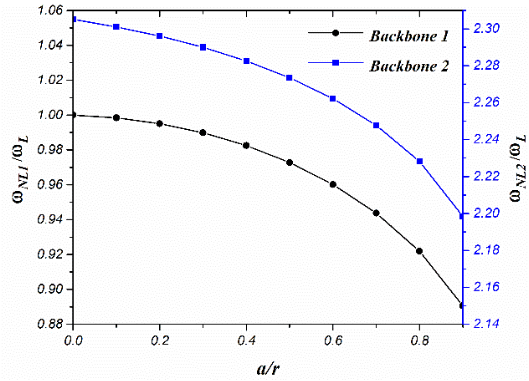

(a) First and second modes

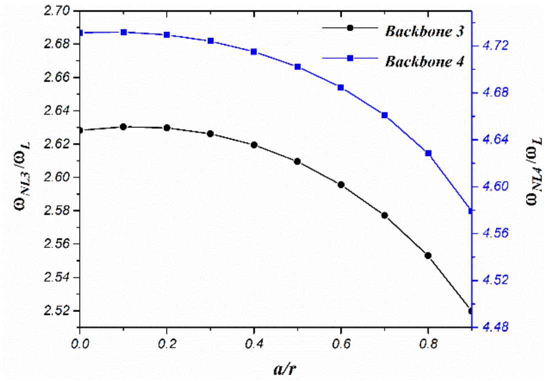

(b) Third and fourth modes

Fig. 18 The backbone curves of the trapezoid dam

that, nonlinear vibration analysis is also performed to achieve the nonlinear frequency ratio. Several values are considered for amplitude vibration (a/r) in which r is the radius of gyration of the cross-section at the free end.

The results are provided for the linear and nonlinear natural frequencies in Table 7, where n is the number of subdivision in each side. In this Table, the comparison of the results is also implemented using the available ones Leung *et al*. (2004). In addition, Fig. 16 shows the convergence study, which is done for this structure.

The first four mode shapes of this structure are demonstrated in Fig. 17. The nonlinear responses are also reported in the form of backbone curves, including the first four nonlinear natural frequencies. These curves are provided in Fig. 18.

5.4 A one-story portal frame

In this part, a one-story plane frame is analyzed. The linear vibration analysis of this problem was investigated by other researchers using beam element (Chen *et al*. 2001). Thus, the authors compare the obtained linear natural frequencies by the reference solutions to show the correctness and high performance of the employed triangular plane element in vibration analysis of skeletal structures with different conditions. The structure's geometry and values of frame's properties are given in Fig. 19.

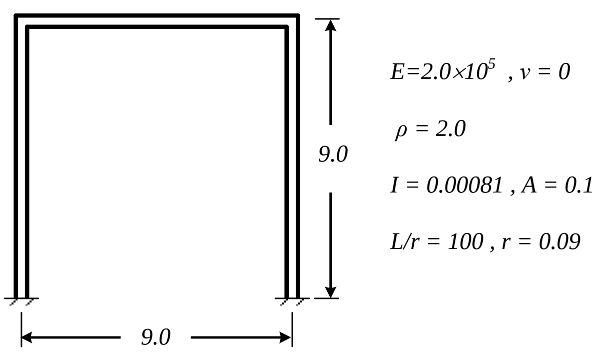

Fig. 19 One-story portal frame

Table 8 The obtained results of linear natural frequencies of the one-story frame

Number of elements	Mode 1	Mode 2	Mode 3	Mode 4
26	1.66712	6.69316	11.30480	13.41672
38	1.64796	6.44140	11.16982	12.40100
124	1.60963	6.28499	10.30587	11.32009

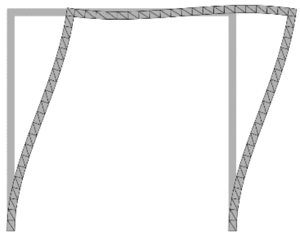

(a) Mode 1

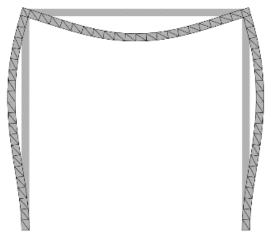

(b) Mode 2

Fig. 20 The mode shapes of one-story frame

where, L and h refer to bay length and height of the frame. The thickness and width of the structure, which are considered for the employed elements are equal to $\frac{5\sqrt{3}}{27}$ and $\frac{9\sqrt{3}}{50}$, respectively. To completely model the frame, 124-triangular elements are employed. The number of elements are specified by using a comparison study between the obtained results of the proposed method and those of other researchers for the first two linear natural frequencies (Chen *et al*. 2001). Table 8 reports the linear natural frequencies of the one-story frame for the different number of elements. The first two mode shapes of structure are also provided in Fig. 20.

Based on the nonlinear vibration results, the corresponded backbone curves are provided in Fig. 21. The large amplitude vibration ratios are assumed to be equal to 0.1 up to 1.5.

5.5 A two-story portal frame

In this example, a two-story plane frame is analyzed

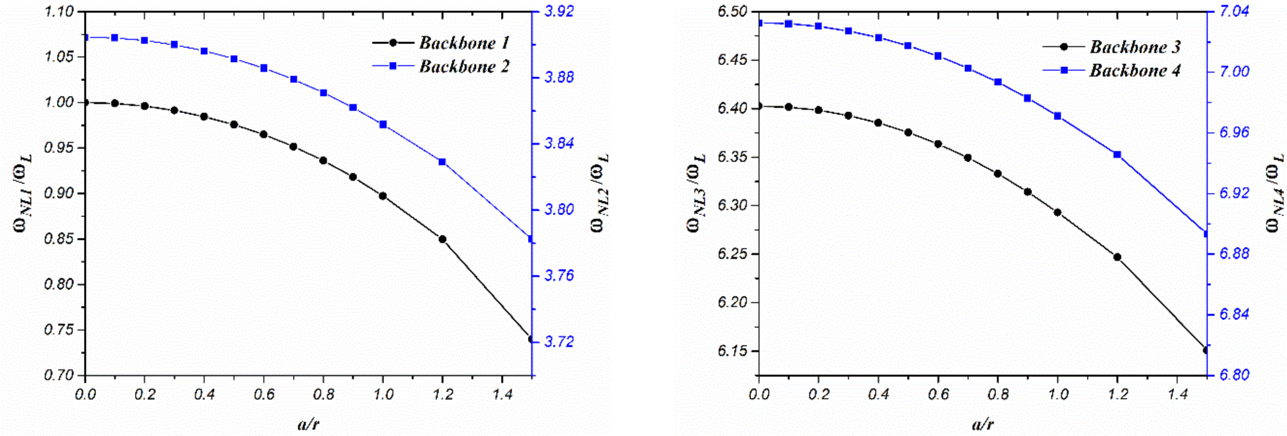

(a) First and second modes (b) Third and fourth modes

Fig. 21 The backbone curves of the one-story portal frame

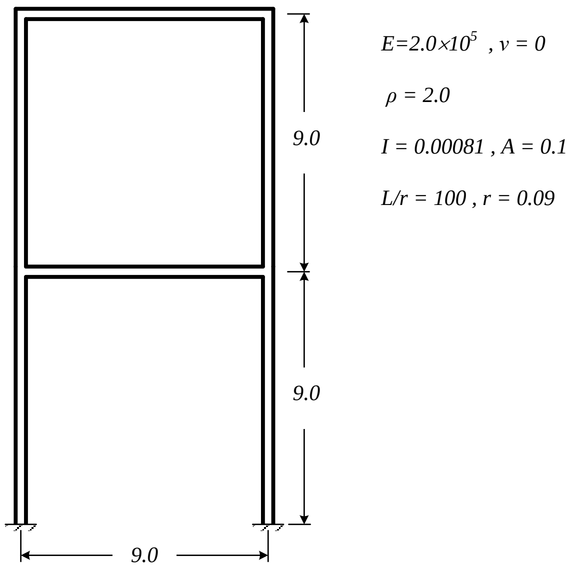

Fig. 22 Two-story plane frame

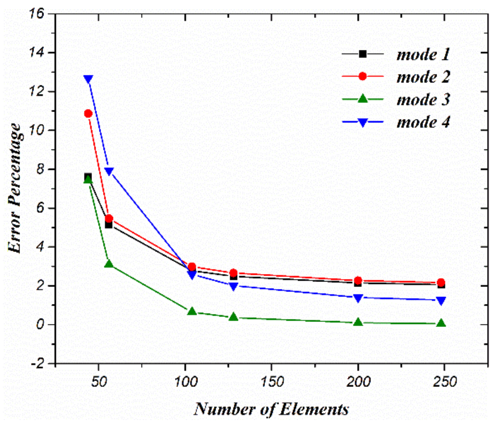

Fig. 23 Convergence study of the two-story portal frame

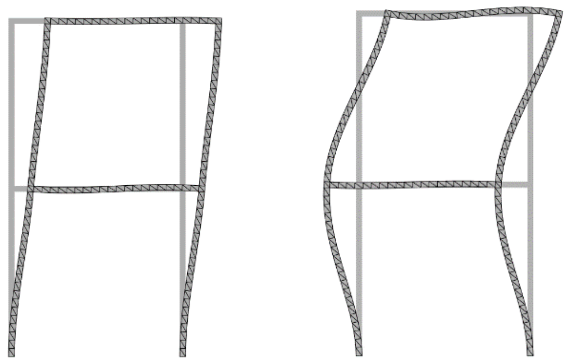

(a) Mode 1 (b) Mode 2

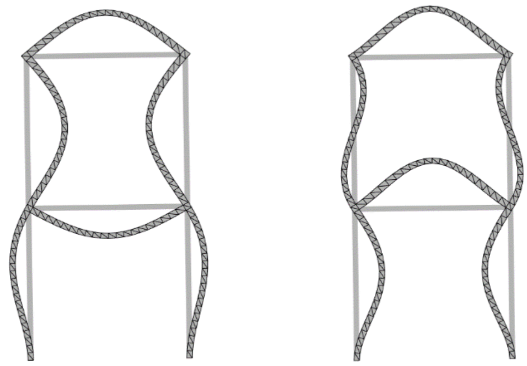

(c) Mode 3 (d) Mode 4

Fig. 24 The mode shapes of two-story portal frame

using the same geometric and mechanical properties, which was presented in section 5.4. The shape of structure is depicted in Fig. 22. This problem with linear behavior was also solved previously (Chen *et al*. 2001). The obtained first four linear natural frequencies are compared with reference solutions. Fig. 23 proves that the error of converging to the accurate results by the new element is negligible.

It is interesting to show the mode shapes of the two-story frame, which is useful to predict the behavior of structure accurately and clearly. Fig. 24 illustrates the first four mode shapes of the frame and the nonlinear responses are reported for different values of the amplitude vibration ratio. This study leads to obtain the backbone curves, shown in Fig. 25 and provided for the ratio of the first four nonlinear natural frequencies to the first linear one.

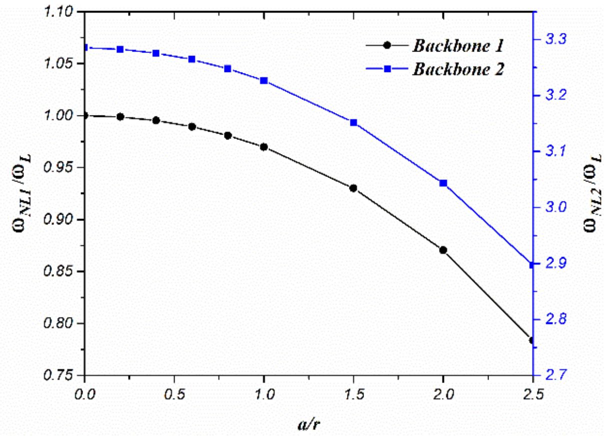

(a) First and second modes

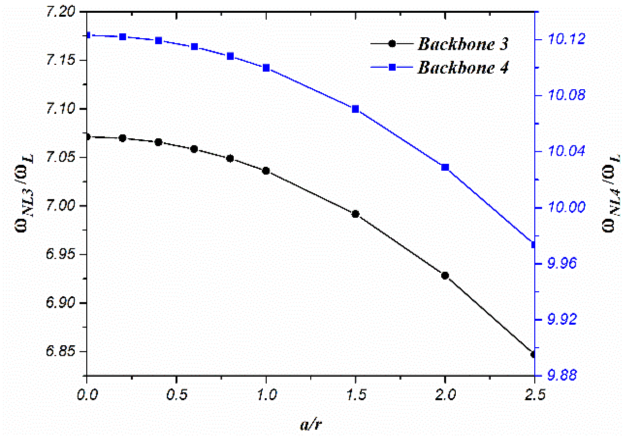

(b) Third and fourth modes

Fig. 25 The backbone curves of the two-story portal frame

5.6 Coupled shear wall

In this part, a four-floor coupled shear wall of Fig. 26 is analyzed. This structure was also analyzed by other researchers (Zhang and Rajendran 2008, Liu *et al*. 2009). The thickness of the shear wall is equal to 1.0 *m*. Moreover the next mechanical and physical properties are assumed

$$E = 10000\ {}^{N}\!/_{m^2} \qquad \nu = 0.2 \qquad \rho = 1.0\ {}^{N}\!/_{m^3}$$

The details of geometric parameters and mesh discretization are presented in Figs. 26-27. In order to reach the optimum mesh, a convergence study is shown in Fig. 28. Moreover, the obtained results for linear and nonlinear vibrations are reported in Table 9.

It is observed that the near exact responses can be achieved by using 144 triangular plane elements, which are employed in this research, while the number of triangular elements used in other investigations were equal to 952 and 3808 (Rajendran and Zhang 2007). This is proven that the proposed element used in this formulation has high performance and accuracy compared to the finite element results of commercial software such as ANSYS and ABAQUS (Liu and Gu 2001a, Rajendran and Zhang2007). To show the behavior of structure in each mode, the linear first four mode shapes of the coupled shear wall are also presented in Fig. 29.

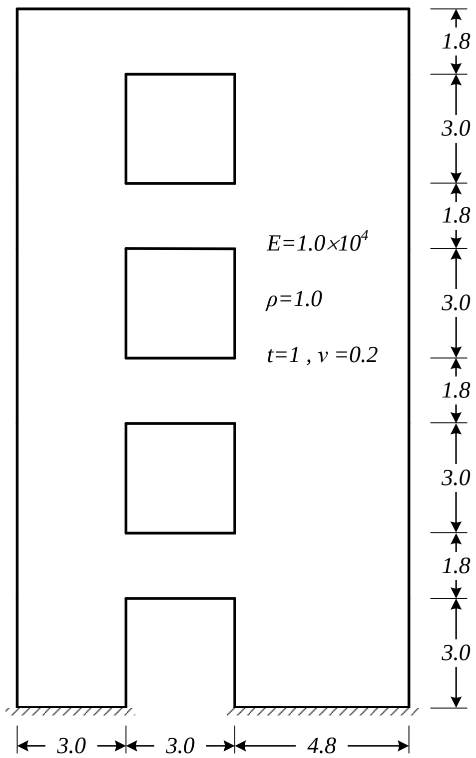

Fig. 26 The geometry of coupled shear wall

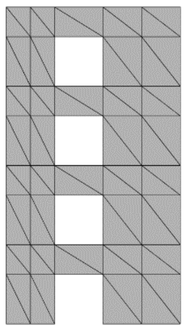

(a) 72 elements

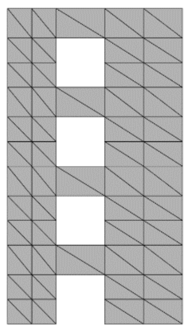

(b) 104 elements

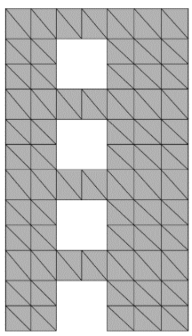

(c) 136 elements

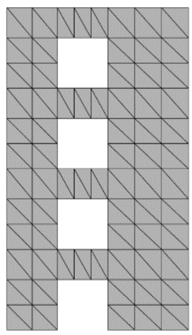

(d) 144 elements

Fig. 27 Different types of mesh discretization

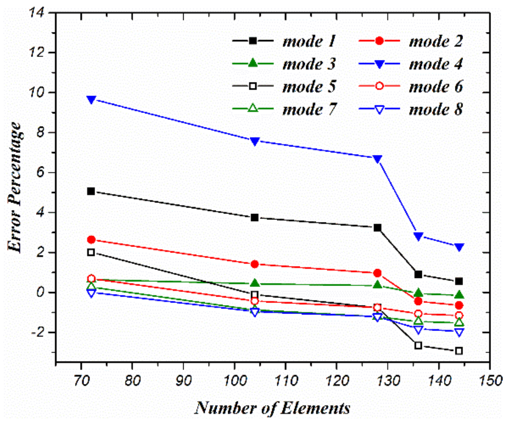

Fig. 28 Convergence study of the coupled shear-wall

Although more elements are required to show the mode shapes smoothly, the authors provided mode shapes of the shear wall using the obtained optimum number of elements equal to 144. Thus, some roughness may be observed in the presented mode shapes, especially in fourth mode. Besides, a nonlinear vibration analysis is implemented to obtain the ratio of nonlinear natural frequency to linear one for the first four modes. Based on the obtained responses, the corresponded backbone curves are provided in Fig. 30.

5.7 Bending of CNTRC beam

This problem is dedicated to investigate the static bending behavior of CNTRC beam. The solution is available, since this beam was also analyzed by other investigators Wattanasakulpong and Ungbhakorn (2013,

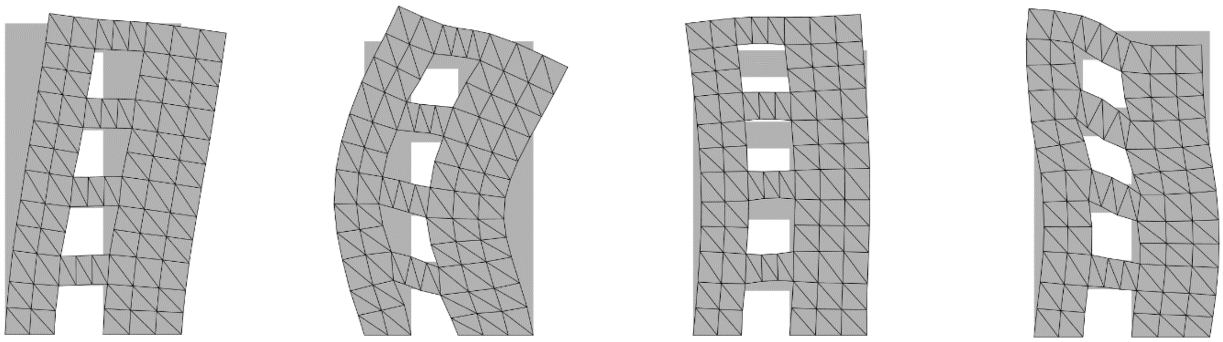

(a) Mode 1 (b) Mode 2 (c) Mode 3 (d) Mode 4

Fig. 29 The mode shapes of coupled shear wall

Table 9 Linear and nonlinear vibrations of the coupled shear wall

$\frac{a}{r}$	$\frac{\omega_{NL}^i}{\omega_L^i}$			
	i = 1	i = 2	i = 3	i = 4
0.0	1.00000	3.41326	3.65156	5.79159
0.1	0.99741	3.41126	3.64822	5.79041
0.2	0.98811	3.39861	3.64441	5.78514
0.3	0.97133	3.37404	3.64031	5.77565
0.4	0.94554	3.33524	3.63609	5.76169
0.5	0.90765	3.27769	3.63194	5.74285
0.6	0.85012	3.19037	3.62834	5.71842
0.7	0.73758	3.02231	3.62759	5.68624

	ω_L^i							
Mode number	i = 1	i = 2	i = 3	i = 4	i = 5	i = 6	i = 7	i = 8
Present	2.0902	7.1345	7.6326	12.11	15.4776	18.4283	19.9578	22.3206
Rajendran and Zhang (2007)	**2.064**	**7.071**	**7.625**	**11.895**	**15.288**	**18.315**	**19.843**	**22.185**
Brebbia and Walker (2016)	**2.079**	**7.181**	**7.644**	**11.833**	**15.947**	**18.644**	**20.268**	**22.765**
Liu and Gu (2001)	**2.086**	**7.152**	**7.647**	**12.019**	**15.628**	**18.548**	**20.085**	**22.564**
ANSYS plane 42 with bubble functions Zhang and Rajendran (2008)	**2.057**	**7.067**	**7.620**	**11.840**	**15.313**	**18.342**	**19.887**	**22.236**
ABAQUS Liu and Gu (2001)	**2.073**	**7.096**	**7.625**	**11.938**	**15.341**	**18.345**	**19.876**	**22.210**

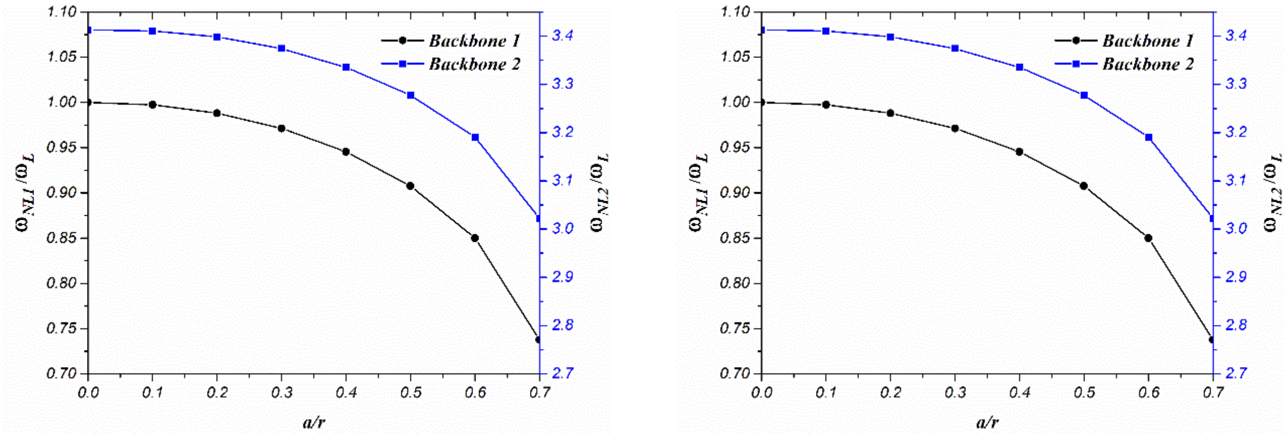

(a) First and second modes

(b) Third and fourth modes

Fig. 30 The backbone curves of the coupled shear-wall

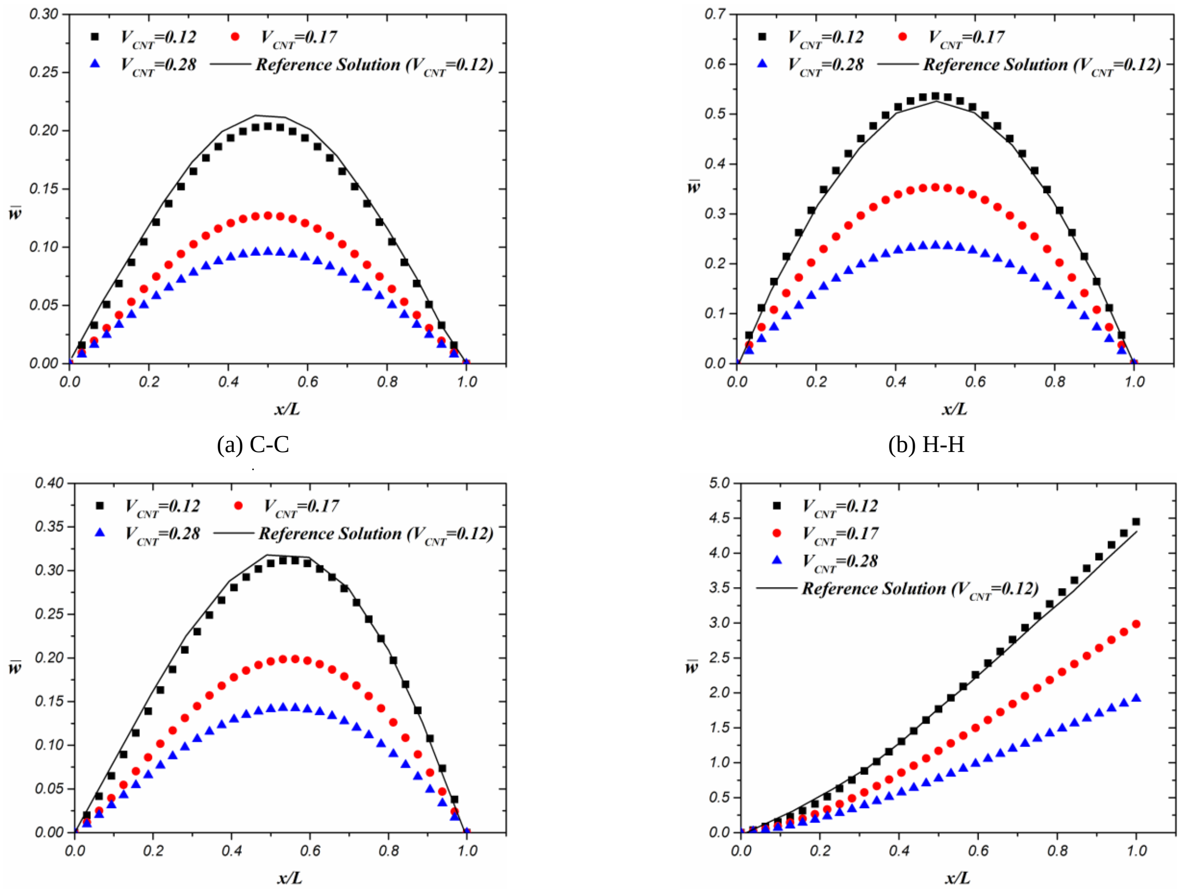

(a) C-C

(b) H-H

(c) C-H

(d) C-F

Fig. 31 The effects of CNT volume fraction factor on the deflection curves of beam with L/h = 15 and $\bar{w} = \frac{100E^m h^3 w(L/2)}{qL^4}$

Kumar and Srinivas (2017). A uniformly distributed load $q = -10^{-5}$ **N/m^2** is applied to along the beam length. The slenderness ratio of the beam is defined by L/h. The width and height of the beam are considered to be the same ($t = h = 1.0$). It is worth mentioning that various boundary conditions, including Clamped-Clamped (C-C), Hinged-Hinged (H-H), Clamped-Free (C-F) and Clamped-Hinged(C-H). In addition, the effects of CNT volume fraction factor (V_{cnt}) and slenderness ratio are also studied. The efficiency factors of CNTs are presented in Table 2. This beam has the following mechanical parameters of material

$$E^m = 2.5\times10^9 \ \mathbf{Pa} \qquad \nu^m = 0.3 \qquad \rho^m = 1190 \ \mathbf{kg/m^3}$$

On the other hand, the properties of SWCNT materials

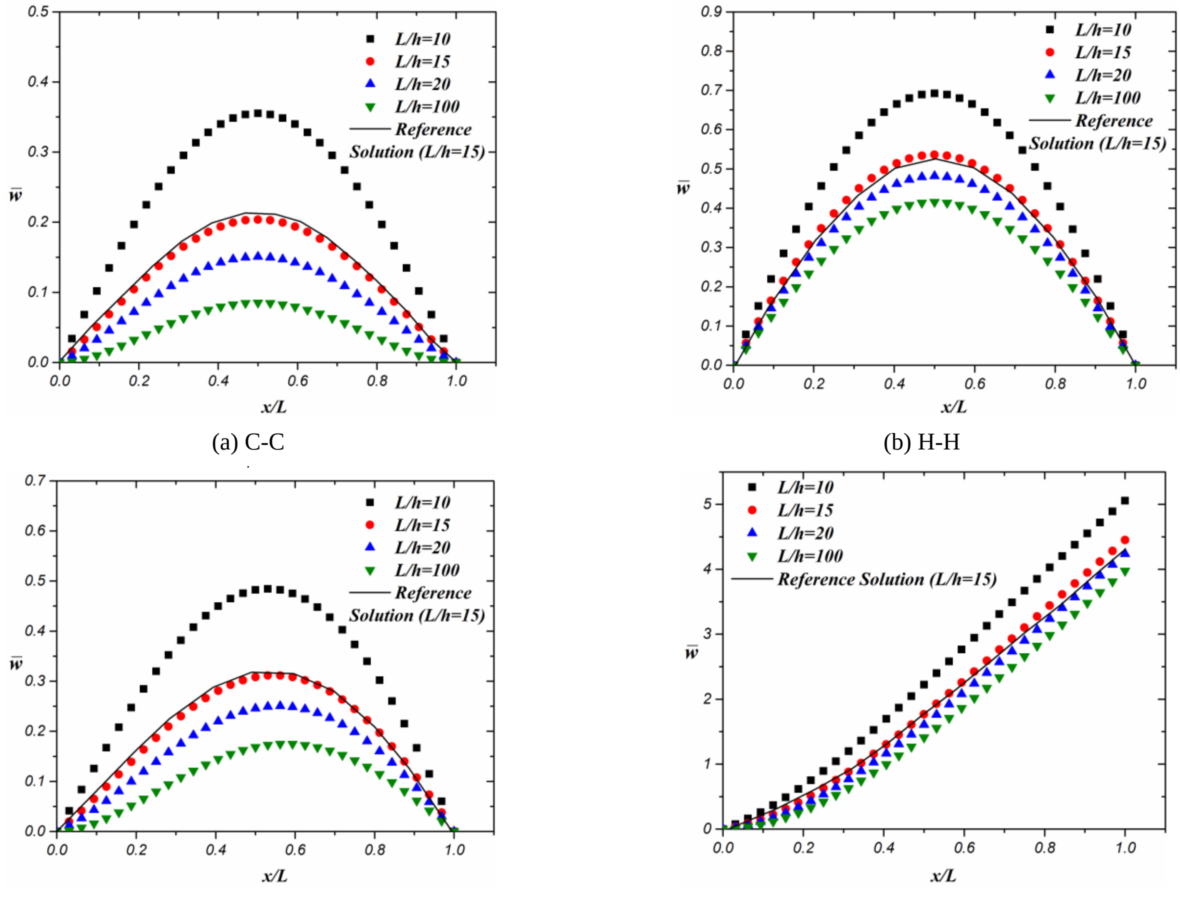

(a) C-C (b) H-H

(c) C-H (d) C-F

Fig. 32 The effects of slenderness ratio on the deflection curves of beam with V_{cnr} = 0.12 and $\bar{w} = \frac{100E^m h^3 w(L/2)}{qL^4}$

at the room temperature (300°K) are considered as follows

$$E_{11}^{cnt} = 6.0\times10^{11} \textbf{ Pa} \qquad E_{22}^{cnt} = 1.0\times10^{10} \textbf{ Pa}$$
$$G_{12}^{cnt} = 1.72\times10^{10} \textbf{ Pa} \qquad \nu^{cnt} = 0.19$$
$$\rho^{cnt} = 1400 \textbf{ kg/m}^3$$

The efficiency parameters associated with the given values of CNT volume fraction are presented in Table 2. By using 32 triangular elements, the CNTRC beam structure, with different slenderness ratio and values of the CNT volume fraction parameters, is modeled. Figs. 31 and 32 provide the deflection curves for the beam. It is noted that the effect of the CNT volume fraction parameters on the structural deflection with different support conditions is investigated in Fig. 31. After solving this problem and for V_{CNT} = 0.12, the results are compared with the available solutions (Kumar and Srinivas 2017a). It is worth mentioning that the slenderness ratio of beam for the obtained results in Fig. 31 is equal to 15.

On the other hand, the influences of the slenderness ratio on the deflection curves of the beam with different boundary conditions are investigated in Fig. 32. It should be noted that the results of Fig. 32 are obtained for V_{CNT} = 0.12. A comparison between obtained responses and reference solutions is observed for the slenderness ratio of 15 in Fig. 32. It is concluded that increasing the volume fraction factor of the CNT reduces the maximum deflection of beam structure in all the cases of support conditions. Based on the obtained responses, the maximum deflection of beam increases by reducing the slenderness ratio of the beam. In other words, the minimum structural deflection is occurred in the case of V_{CNT} = 0.28 and L/h = 100.

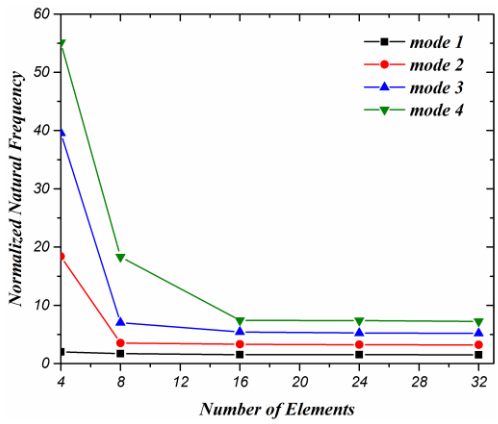

Fig. 33 The convergence study of linear natural frequencies of CNTRC beam

5.8 Vibration of CNTRC beam problem

This example is dedicated to investigate the vibration responses of a CNTRC beam. All geometric and material properties of this structure are the same as the previous problem. It should be added that this problem is solved in the other researches (Kumar and Srinivas 2017a). After solving this structure, the results are employed for

Table 10 The dimensionless frequency parameter of beam for V_{cnr} = 0.12

BCs	Mode number		$\frac{L}{h}=15$	$\frac{L}{h}=20$	$\frac{L}{h}=100$
C-C	$\bar{\omega}_1$	Present	1.5122	1.3310	0.3679
		Kumar and Srinivas (2017)	1.5874	---------	---------
		Yas and Samadi (2012)	1.5085	---------	---------
	$\bar{\omega}_2$	Present	3.1989	2.9324	0.9921
		Kumar and Srinivas (2017)	3.3314	---------	---------
		Yas and Samadi (2012)	3.1353	---------	---------
	$\bar{\omega}_3$	Present	5.1504	4.8095	1.8923
		Kumar and Srinivas (2017)	5.4075	---------	---------
		Yas and Samadi (2012)	4.9979	---------	---------
	$\bar{\omega}_4$	Present	7.1707	6.7952	3.0293
		Kumar and Srinivas (2017)	7.6482	---------	---------
H-H	$\bar{\omega}_1$	Present	0.9419	0.7530	0.1648
		Kumar and Srinivas (2017)	1.0247	---------	---------
		Yas and Samadi (2012)	0.9753	---------	---------
	$\bar{\omega}_2$	Present	2.8158	2.4561	0.6515
		Kumar and Srinivas (2017)	3.0473	---------	---------
		Yas and Samadi (2012)	2.8728	---------	---------
	$\bar{\omega}_3$	Present	4.8423	4.4483	1.4386
		Kumar and Srinivas (2017)	5.2566	---------	---------
		Yas and Samadi (2012)	4.8704	---------	---------
	$\bar{\omega}_4$	Present	6.8771	6.5012	2.4943
		Kumar and Srinivas (2017)	7.5561	---------	---------
C-H	$\bar{\omega}_1$	Present	1.2269	1.0379	0.2557
		Kumar and Srinivas (2017)	1.3087	---------	---------
		Yas and Samadi (2012)	1.2444	---------	---------
	$\bar{\omega}_2$	Present	3.0185	2.7076	0.8148
		Kumar and Srinivas (2017)	3.2019	---------	---------
		Yas and Samadi (2012)	3.0159	---------	---------
	$\bar{\omega}_3$	Present	4.9970	4.6328	1.6609
		Kumar and Srinivas (2017)	5.3319	---------	---------
		Yas and Samadi (2012)	4.9342	---------	---------
	$\bar{\omega}_4$	Present	7.0237	6.6500	2.7598
		Kumar and Srinivas (2017)	7.6032	---------	---------
C-F	$\bar{\omega}_1$	Present	0.3635	0.2816	0.0658
		Kumar and Srinivas (2017)	0.3947	---------	---------
	$\bar{\omega}_2$	Present	1.6881	1.4388	0.3646
		Kumar and Srinivas (2017)	1.7899	---------	---------
	$\bar{\omega}_3$	Present	3.6948	3.2981	1.0038
		Kumar and Srinivas (2017)	3.9010	---------	---------
	$\bar{\omega}_4$	Present	5.7678	5.3227	1.9207
		Kumar and Srinivas (2017)	6.1165	---------	---------

comparison study. Two parameters, including slenderness ratio and volume fraction of CNT factor are studied in this part separately. A convergence study is performed to reach the optimum number of triangular elements. Fig. 33 shows the convergence curves for the first four modes of vibration. For this purpose, the slenderness ratio and volume fraction factor are assumed to be L/h = 15 and V_{CNT} = 0.12. In this example, the boundary condition of the beam is considered

Table 11 The dimensionless frequency parameter of beam for V_{cnr} = 0.17

BCs	Mode number		$\frac{L}{h}=15$	$\frac{L}{h}=20$	$\frac{L}{h}=100$
C-C	$\bar{\omega}_1$	Present	1.9108	1.6648	0.4451
		Kumar and Srinivas (2017)	2.0130	---------	---------
		Yas and Samadi (2012)	1.9144	---------	---------
	$\bar{\omega}_2$	Present	4.0807	3.7140	1.2039
		Kumar and Srinivas (2017)	4.2652	---------	---------
		Yas and Samadi (2012)	4.0187	---------	---------
	$\bar{\omega}_3$	Present	6.5992	6.1277	2.3048
		Kumar and Srinivas (2017)	6.9521	---------	---------
		Yas and Samadi (2012)	6.4348	---------	---------
	$\bar{\omega}_4$	Present	9.2211	8.6962	3.7045
		Kumar and Srinivas (2017)	9.8692	---------	---------
H-H	$\bar{\omega}_1$	Present	1.1585	0.9196	0.1989
		Kumar and Srinivas (2017)	1.2603	---------	---------
		Yas and Samadi (2012)	1.1999	---------	---------
	$\bar{\omega}_2$	Present	3.5456	3.0604	0.7878
		Kumar and Srinivas (2017)	3.8439	---------	---------
		Yas and Samadi (2012)	3.6276	---------	---------
	$\bar{\omega}_3$	Present	6.1736	5.6219	1.7442
		Kumar and Srinivas (2017)	6.7213	---------	---------
		Yas and Samadi (2012)	6.2363	---------	---------
	$\bar{\omega}_4$	Present	8.8239	8.2861	3.0343
		Kumar and Srinivas (2017)	9.7284	---------	---------
C-H	$\bar{\omega}_1$	Present	1.5337	1.2846	0.3090
		Kumar and Srinivas (2017)	1.6396	---------	---------
		Yas and Samadi (2012)	1.5602	---------	---------
	$\bar{\omega}_2$	Present	3.8285	3.4044	0.9870
		Kumar and Srinivas (2017)	4.0722	---------	---------
		Yas and Samadi (2012)	3.8402	---------	---------
	$\bar{\omega}_3$	Present	6.3880	5.8809	2.0183
		Kumar and Srinivas (2017)	6.8375	---------	---------
		Yas and Samadi (2012)	6.3370	---------	---------
	$\bar{\omega}_4$	Present	9.0226	8.4939	3.3660
		Kumar and Srinivas (2017)	9.8003	---------	---------
C-F	$\bar{\omega}_1$	Present	0.4431	0.3419	0.0710
		Kumar and Srinivas (2017)	0.4810	---------	---------
	$\bar{\omega}_2$	Present	2.1137	1.7849	0.4408
		Kumar and Srinivas (2017)	2.2470	---------	---------
	$\bar{\omega}_3$	Present	4.6804	4.1455	1.2163
		Kumar and Srinivas (2017)	4.9553	---------	---------
	$\bar{\omega}_4$	Present	7.3682	6.7540	2.3348
		Kumar and Srinivas (2017)	7.8387	---------	---------

to be Clamped-Clamped.

As it is shown in Tables 10-12, the linear natural frequencies of the beam are obtained for different values of the slenderness ratio (15, 20 and 100). It is observed that the natural frequencies are reported in the normalized form as follows

$$\bar{\omega} = \omega L \sqrt{\frac{I}{A}} = \omega L \sqrt{\frac{\rho_m (1-\nu_m^2)}{E_m}} \tag{26}$$

Table 12 The dimensionless frequency parameter of beam for V_{cnr} = 0.28

BCs	Mode number		$\frac{L}{h}=15$	$\frac{L}{h}=20$	$\frac{L}{h}=100$
C-C	$\bar{\omega}_1$	Present	2.1697	1.9318	0.5566
		Kumar and Srinivas (2017)	2.2631	---------	---------
		Yas and Samadi (2012)	2.1618	---------	---------
	$\bar{\omega}_2$	Present	4.5451	4.1982	1.4947
		Kumar and Srinivas (2017)	4.7070	---------	---------
		Yas and Samadi (2012)	4.4556	---------	---------
	$\bar{\omega}_3$	Present	7.2828	6.8424	2.8377
		Kumar and Srinivas (2017)	7.6087	---------	---------
		Yas and Samadi (2012)	7.0745	---------	---------
	$\bar{\omega}_4$	Present	10.0993	9.6205	4.5192
		Kumar and Srinivas (2017)	10.7218	---------	---------
H-H	$\bar{\omega}_1$	Present	1.3945	1.1252	0.2501
		Kumar and Srinivas (2017)	1.5097	---------	---------
		Yas and Samadi (2012)	1.4401	---------	---------
	$\bar{\omega}_2$	Present	4.0534	3.5797	0.9864
		Kumar and Srinivas (2017)	4.3677	---------	---------
		Yas and Samadi (2012)	4.1362	---------	---------
	$\bar{\omega}_3$	Present	6.8752	6.3787	2.1704
		Kumar and Srinivas (2017)	7.4327	---------	---------
		Yas and Samadi (2012)	6.9245	---------	---------
	$\bar{\omega}_4$	Present	9.6961	9.2363	3.7464
		Kumar and Srinivas (2017)	10.6136	---------	---------
C-H	$\bar{\omega}_1$	Present	1.7819	1.5253	0.3875
		Kumar and Srinivas (2017)	1.8892	---------	---------
		Yas and Samadi (2012)	1.8040	---------	---------
	$\bar{\omega}_2$	Present	4.3135	3.9071	1.2309
		Kumar and Srinivas (2017)	4.5533	---------	---------
		Yas and Samadi (2012)	4.3112	---------	---------
	$\bar{\omega}_3$	Present	7.0789	6.6146	2.4985
		Kumar and Srinivas (2017)	7.5197	---------	---------
		Yas and Samadi (2012)	6.9987	---------	---------
	$\bar{\omega}_4$	Present	9.8970	9.4303	4.1313
		Kumar and Srinivas (2017)	10.6691	---------	---------
C-F	$\bar{\omega}_1$	Present	0.5446	0.4242	0.0893
		Kumar and Srinivas (2017)	0.5878	---------	---------
	$\bar{\omega}_2$	Present	2.4485	2.1091	0.5524
		Kumar and Srinivas (2017)	2.5799	---------	---------
	$\bar{\omega}_3$	Present	5.2901	4.7632	1.5157
		Kumar and Srinivas (2017)	5.5557	---------	---------
	$\bar{\omega}_4$	Present	8.1813	7.6053	2.8879
		Kumar and Srinivas (2017)	8.6321	---------	---------

These responses are provided for various states of support conditions, including C-C, H-H, C-H and C-F. It is worth mentioning that the volume fraction factor changes for each Table.

6. Conclusions

To analyze the UD-CNTRC and homogenous structures, considering geometric nonlinearity, an efficient plane triangular element was formulated. The related eigenvalue problem was solved to achieve the natural frequencies. To obtain nonlinear natural frequencies, by using a novel mixed interpolated tensorial finite element method procedure, large amplitude vibration analysis was implemented. It is worth mentioning that the first mode shape of the structure was selected to apply as initial deformation for geometrically nonlinear analysis. To considering large displacements, Total Lagrangian formulation was utilized. On the other hand, locking phenomena occurrence was prevented by using MITC method. The authors solved several benchmark problems to show the accuracy and capability of their scheme. Obtained results are in good agreement with those of the pervious researches with more degrees of freedom. That's while the number of degrees of freedom, used in this research, is considerably less than the other ones. In addition, some new plane problems were analyzed to indicate the high performance of proposed formulation in obtaining the linear and nonlinear vibration responses of homogenous and UD-CNTRC's plane structures.

Funding

This study was not funded by any company.

Conflict of interest

The authors declare that they have no conflict of interest

References

Alijani, F. and Amabili, M. (2014), “Non-linear vibrations of shells: A literature review from 2003 to 2013”, *Int. J. Non-Linear Mech.*, **58**, 233-257.

Allahkarami, F., Nikkhah-Bahrami, M. and Saryazdi, M.G. (2018), “Nonlinear forced vibration of FG-CNTs-reinforced curved microbeam based on strain gradient theory considering out-of-plane motion”, *Steel Compos. Struct., Int. J.*, **26**(6), 673-691.

Allaoui, A., Bai, S., Cheng, H.-M. and Bai, J. (2002), “Mechanical and electrical properties of a MWNT/epoxy composite”, *Compos. Sci. Technol.*, **62**(15), 1993-1998.

Allman, D. (1984), “A compatible triangular element including vertex rotations for plane elasticity analysis”, *Comput. Struct.*, **19**(1-2), 1-8.

Amabili, M. (2017), “Nonlinear damping in large-amplitude vibrations: modelling and experiments”, *Nonlinear Dyn.*, 1-14.

Ansari, R. and Hemmatnezhad, M. (2012), “Nonlinear finite element analysis for vibrations of double-walled carbon nanotubes”, *Nonlinear Dyn.*, **67**(1), 373-383.

Bergan, P. and Felippa, C.A. (1985), “A triangular membrane element with rotational degrees of freedom”, *Comput. Methods Appl. Mech. Eng.*, **50**(1), 25-69.

Bhashyam, G. and Prathap, G. (1980), “Galerkin finite element method for non-linear beam vibrations”, *J. Sound Vib.*, **72**(2), 191-203.

Billings, S.A. (2013), *Nonlinear system identification: NARMAX methods in the time, frequency, and spatio-temporal domains*, John Wiley & Sons.

Brebbia, C.A. and Walker, S. (2016), *Boundary Element Techniques in Engineering*, Elsevier.

Caliò, I. and Greco, A. (2014), “Free vibrations of spatial Timoshenko arches”, *J. Sound Vibr.*, **333**(19), 4543-4561.

Chavan, S.G. and Lal, A. (2017), “Bending behavior of SWCNT reinforced composite plates”, *Steel Compos. Struct., Int. J.*, **24**(5), 537-548.

Chen, S., Cheung, Y. and Xing, H. (2001), “Nonlinear vibration of plane structures by finite element and incremental harmonic balance method”, *Nonlinear Dyn.*, **26**(1), 87-104.

Ding, H., Zhu, M.-H. and Chen, L.-Q. (2018), “Nonlinear vibration isolation of a viscoelastic beam”, *Nonlinear Dyn.*, **92**(2), 325-349.

Dumir, P. and Bhaskar, A. (1988), “Some erroneous finite element formulations of non-linear vibrations of beams and plates”, *J. Sound Vib.*, **123**(3), 517-527.

Erik, T.T. and Chou, T.W. (2002), “Aligned multi-walled carbon nanotube-reinforced composites: processing and mechanical characterization”, *J. Phys. D: Appl. Phys.*, **35**(16), L77.

Fajman, P. (2002), “New triangular plane element with drilling degrees of freedom”, *J. Eng. Mech.*, **128**(4), 413-418.

Felippa, C.A. (2003), “A study of optimal membrane triangles with drilling freedoms”, *Comput. Methods Appl. Mech. Eng.*, **192**(16-18), 2125-2168.

Feng, Y. and Bert, C.W. (1992), “Application of the quadrature method to flexural vibration analysis of a geometrically nonlinear beam”, *Nonlinear Dyn.*, **3**(1), 13-18.

Gupta, K. (1978), “Development of a finite dynamic element for free vibration analysis of two-dimensional structures”, *Int. J. Numer. Methods Eng.*, **12**(8), 1311-1327.

Gupta, K.K. (1979), “Finite dynamic element formulation for a plane triangular element”, *Int. J. Numer. Methods Eng.*, **14**(10), 1431-1448.

Heydari, M.M., Hafizi Bidgoli, A., Golshani, H.R., Beygipoor, G. and Davoodi, A. (2015), “Nonlinear bending analysis of functionally graded CNT-reinforced composite Mindlin polymeric temperature-dependent plate resting on orthotropic elastomeric medium using GDQM”, *Nonlinear Dyn.*, **79**(2), 1425-1441.

Hirwani, C.K. and Panda, S.K. (2018), “Numerical nonlinear frequency analysis of pre-damaged curved layered composite structure using higher-order finite element method”, *Int. J. Non-Linear Mech.*, **102**, 14-24.

Hirwani, C., Mahapatra, T., Panda, S., Sahoo, S., Singh, V. and Patle, B. (2017), “Nonlinear free vibration analysis of laminated carbon/epoxy curved panels”, *Defence Sci. J.*, **67**(2), 207.

Iu, V., Cheung, Y. and Lau, S. (1985), “Non-linear vibration analysis of multilayer beams by incremental finite elements, Part I: Theory and numerical formulation”, *J. Sound Vib*, **100**(3), 359-372.

Kolahdouzan, F., Arani, A.G. and Abdollahian, M. (2018), “Buckling and free vibration analysis of FG-CNTRC-micro sandwich plate”, *Steel Compos. Struct., Int. J.*, **26**(3), 273-287.

Kumar, P. and Srinivas, J. (2017a), “Free vibration, bending and buckling of a FG-CNT reinforced composite beam: Comparative analysis with hybrid laminated composite beam”, *Multidiscipl. Model. Mater. Struct.*, **13**(4), 590-611.

Kumar, P. and Srinivas, J. (2017b), “Vibration, buckling and bending behavior of functionally graded multi-walled carbon nanotube reinforced polymer composite plates using the layer-wise formulation”, *Compos. Struct.*, **177**, 158-170.

Leung, A. and Fung, T. (1989), “Non-linear steady state vibration of frames by finite element method”, *Int. J. Numer. Methods Eng.*, **28**(7), 1599-1618.

Leung, A., Zhu, B., Zheng, J. and Yang, H. (2004), “Analytic trapezoidal Fourier p-element for vibrating plane problems”, *J. Sound Vib.*, **271**(1-2), 67-81.

Lewandowski, R. (1994), “Non-linear free vibrations of beams by the finite element and continuation methods”, *J. Sound Vib.*, **170**(5), 577-593.

Liew, K., Rajendran, S. and Wang, J. (2006), “A quadratic plane triangular element immune to quadratic mesh distortions under quadratic displacement fields”, *Comput. Methods Appl. Mech. Eng.*, **195**(9-12), 1207-1223.

Liew, K., Lei, Z. and Zhang, L. (2015), “Mechanical analysis of functionally graded carbon nanotube reinforced composites: a review”, *Compos. Struct.*, **120**, 90-97.

Lin, F. and Xiang, Y. (2014a), “Numerical analysis on nonlinear free vibration of carbon nanotube reinforced composite beams”, *Int. J. Struct. Stabil. Dyn.*, **14**(1), 1350056.

Lin, F. and Xiang, Y. (2014b), “Vibration of carbon nanotube reinforced composite beams based on the first and third order beam theories”, *Appl. Math. Model.*, **38**(15-16), 3741-3754.

Liu, G.-R. and Gu, Y. (2001a), “A point interpolation method for two-dimensional solids”, *Int. J. Numer. Methods Eng.*, **50**(4), 937-951.

Liu, G. and Gu, Y. (2001b), “A local radial point interpolation method (LRPIM) for free vibration analyses of 2-D solids”, Journal of Sound and Vibration, **246**(1), 29-46.

Liu, G., Nguyen-Thoi, T. and Lam, K. (2009), “An edge-based smoothed finite element method (ES-FEM) for static, free and forced vibration analyses of solids”, *J. Sound Vib.*, **320**(4-5), 1100-1130.

Mahapatra, T.R., Mehar, K., Panda, S.K., Dewangan, S. and Dash, S. (2017), “Flexural strength of functionally graded nanotube reinforced sandwich spherical panel”, *IOP Conference Series: Materials Science and Engineering*, IOP Publishing.

Marur, S. and Prathap, G. (2005), “Non-linear beam vibration problems and simplifications in finite element models”, *Computat. Mech.*, **35**(5), 352-360.

Masoodi, A.R. and Arabi, E. (2018), “Geometrically nonlinear thermomechanical analysis of shell-like structures”, *J. Thermal Stress.*, **41**(1), 37-53.

Mayandi, K. and Jeyaraj, P. (2015), “Bending, buckling and free vibration characteristics of FG-CNT-reinforced polymer composite beam under non-uniform thermal load”, *Proceedings of the Institution of Mechanical Engineers, Part L: Journal of Materials: Design and Applications*, **229**(1), 13-28.

Mehar, K. and Panda, S.K. (2016a), “Free vibration and bending behaviour of CNT reinforced composite plate using different shear deformation theory”, *IOP Conference Series: Materials Science and Engineering*, IOP Publishing.

Mehar, K. and Panda, S.K. (2016b), “Geometrical nonlinear free vibration analysis of FG-CNT reinforced composite flat panel under uniform thermal field”, *Compos. Struct.*, **143**, 336-346.

Mehar, K. and Panda, S.K. (2016c), “Nonlinear static behavior of FG-CNT reinforced composite flat panel under thermomechanical load”, *J. Aerosp. Eng.*, **30**(3), 04016100.

Mehar, K. and Panda, S.K. (2017), “Thermoelastic analysis of FG-CNT reinforced shear deformable composite plate under various loadings”, *Int. J. Computat. Methods*, **14**(2), 1750019.

Mehar, K. and Panda, S.K. (2018a), “Elastic bending and stress analysis of carbon nanotube-reinforced composite plate: Experimental, numerical, and simulation”, *Adv. Polym. Technol.*, **37**(6), 1643-1657.

Mehar, K. and Panda, S.K. (2018b), “Thermal free vibration behavior of FG-CNT reinforced sandwich curved panel using finite element method”, *Polym. Compos.*, **39**(8), 2751-2764.

Mehar, K. and Panda, S.K. (2018c), “Nonlinear finite element solutions of thermoelastic flexural strength and stress values of temperature dependent graded CNT-reinforced sandwich shallow shell structure”, *Struct. Eng. Mech., Ing. J.*, **67**(6), 565-578.

Mehar, K., Panda, S.K., Dehengia, A. and Kar, V.R. (2016), “Vibration analysis of functionally graded carbon nanotube reinforced composite plate in thermal environment”, *J. Sandw. Struct. Mater.*, **18**(2), 151-173.

Mehar, K., Panda, S.K. and Mahapatra, T.R. (2017a), “Theoretical and experimental investigation of vibration characteristic of carbon nanotube reinforced polymer composite structure”, *Int. J. Mech. Sci.*, **133**, 319-329.

Mehar, K., Panda, S.K. and Mahapatra, T.R. (2017b), “Thermo-elastic nonlinear frequency analysis of CNT reinforced functionally graded sandwich structure”, *Eur. J. Mech.-A/Solids*, **65**, 384-396.

Mehar, K., Panda, S.K. and Mahapatra, T.R. (2018a), “Nonlinear Frequency Responses of Functionally Graded Carbon Nanotube-Reinforced Sandwich Curved Panel Under Uniform Temperature Field”, *Int. J. Appl. Mech.*, **10**(3), 1850028.

Mehar, K., Panda, S.K. and Mahapatra, T.R. (2018b), “Thermo-elastic deflection responses of CNT reinforced sandwich shell structure using finite element method”, *Scientia Iranica*, **25**(5), 2722-2737.

Mehar, K., Panda, S.K. and Patle, B.K. (2018c), “Stress, deflection, and frequency analysis of CNT reinforced graded sandwich plate under uniform and linear thermal environment: A finite element approach”, *Polym. Compos.*, **39**(10), 3792-3809.

Mei, C. (1972), “Nonlinear vibration of beams by matrix displacement method”, *AIAA Journal*, **10**(3), 355-357.

Mei, C. (1973), “Finite element displacement method for large amplitude free flexural vibrations of beams and plates”, *Comput. Struct.*, **3**(1), 163-174.

Mei, C. (1986), “Discussion of finite element formulations of nonlinear beam vibrations”, *Comput. Struct.*, **22**(1), 83-85.

Mir, M., Tahani, M. and Hassani, B. (2017), “Analytical prediction of Young’s modulus of carbon nanotubes using a variational method”, *Appl. Math. Model.*, **45**, 1031-1043.

Mohamed, N., Eltaher, M.A., Mohamed, S.A. and Seddek, L.F. (2018), “Numerical analysis of nonlinear free and forced vibrations of buckled curved beams resting on nonlinear elastic foundations”, *Int. J. Non-Linear Mech.*, **101**, 157-173.

Qaisi, M. (1997), “A power series solution for the non-linear vibration of beams”, *J. Sound Vib.*, **199**(4), 587-594.

Rajendran, S. and Zhang, B. (2007), “A “FE-meshfree” QUAD4 element based on partition of unity”, *Comput. Methods Appl. Mech. Eng.*, **197**(1-4), 128-147.

Rao, S.S. (2007), *Vibration of Continuous Systems*, John Wiley & Sons.

Rao, G.V. and Raju, K.K. (2003), “Large amplitude free vibrations of beams–an energy approach”, *ZAMM-Journal of Applied Mathematics and Mechanics/Zeitschrift für Angewandte Mathematik und Mechanik*, **83**(7), 493-498.

Rehfield, L.W. (1973), “Nonlinear free vibrations of elastic structures”, *Int. J. Solids Struct.*, **9**(5), 581-590.

Rezaiee-Pajand, M. and Masoodi, A.R. (2016), “Exact natural frequencies and buckling load of functionally graded material tapered beam-columns considering semi-rigid connections”, *J. Vib. Control*, **24**(9), 1787-1808.

Rezaiee-Pajand, M. and Rajabzadeh-Safaei, N. (2016a), “An explicit stiffness matrix for parabolic beam element”, *Latin Am.*

J. Solids Struct., **13**, 1782-1801.

Rezaiee Pajand, M. and Rajabzadeh Safaei, N. (2016b), “Static and dynamic analysis of circular beams using explicit stiffness matrix”, *Struct. Eng. Mech., Ing. J.*, **60**(1), 111-130.

Rezaiee-Pajand, M. and Yaghoobi, M. (2014), “An efficient formulation for linear and geometric non-linear membrane elements”, *Latin Am. J. Solids Struct.*, **11**(6), 1012-1035.

Rezaiee-Pajand, M., Arabi, E. and Masoodi, A.R. (2018a), “A triangular shell element for geometrically nonlinear analysis”, *Acta Mechanica*, **229**(1), 323-342.

Rezaiee-Pajand, M., Mokhtari, M. and Masoodi, A.R. (2018b), “Stability and free vibration analysis of tapered sandwich columns with functionally graded core and flexible connections”, *CEAS Aeronaut. J.*, **9**(4), 629-648.

Rezaiee-Pajand, M., Rajabzadeh-Safaei, N. and Hozhabrossadati, S.M. (2018d), “Three-dimensional deformations of a curved circular beam subjected to thermo-mechanical loading using green’s function method”, *Int. J. Mech. Sci.*, **142-143**, 163-175.

Rezaiee Pajand, M., Masoodi, A. and Arabi, E. (2018e), “Geometrically nonlinear analysis of FG doubly-curved and hyperbolical shells via laminated by new element”, *Steel Compos. Struct., Int. J.*, **28**(3), 389-401.

Rezaiee-Pajand, M., Arabi, E. and Masoodi, A.R. (2019), “Nonlinear analysis of FG-sandwich plates and shells”, *Aerosp. Sci. Technol.* [In Press]

Sadri, M., Younesian, D. and Esmailzadeh, E. (2016), “Nonlinear harmonic vibration and stability analysis of a cantilever beam carrying an intermediate lumped mass”, *Nonlinear Dyn.*, **84**(3), 1667-1682.

Salvetat, J.-P., Bonard, J.-M., Thomson, N.H., Kulik, A.J., Forró, L., Benoit, W. and Zuppiroli, L. (1999), “Mechanical properties of carbon nanotubes”, *Appl. Phys. A*, **69**(3), 255-260.

Sarma, B. and Varadan, T. (1982), “Certain discussions in the finite element formulation of nonlinear vibration analysis”, *Comput. Struct.*, **15**(6), 643-646.

Sarma, B., Varadan, T. and Prathap, G. (1988), “On various formulations of large amplitude free vibrations of beams”, *Comput. Struct.*, **29**(6), 959-966.

Shafiei, H. and Setoodeh, A.R. (2017), “Nonlinear free vibration and post-buckling of FG-CNTRC beams on nonlinear foundation”, *Steel Compos. Struct., Int. J.*, **24**, 65-77.

Shang, H.Y., Machado, R.D., Abdalla Filho, J.E. and Arndt, M. (2017), “Numerical analysis of plane stress free vibration in severely distorted mesh by Generalized Finite Element Method”, *Eur. J. Mech.-A/Solid*s, **62**, 50-66.

Shen, H.-S. (2009), “Nonlinear bending of functionally graded carbon nanotube-reinforced composite plates in thermal environments”, *Compos. Struct.*, **91**(1), 9-19.

Shen, H.-S., Lin, F. and Xiang, Y. (2017), “Nonlinear vibration of functionally graded graphene-reinforced composite laminated beams resting on elastic foundations in thermal environments”, *Nonlinear Dyn.*, **90**(2), 899-914.

Singh, G., Rao, G.V. and Iyengar, N. (1990a), “Re-investigation of large-amplitude free vibrations of beams using finite elements”, *J. Sound Vib.*, **143**(2), 351-355.

Singh, G., Sharma, A. and Rao, G.V. (1990b), “Large-amplitude free vibrations of beams—a discussion on various formulations and assumptions”, *J. Sound Vib.*, **142**(1), 77-85.

Tahouneh, V. (2017), “Vibration and mode shape analysis of sandwich panel with MWCNTs FG-reinforcement core”, *Steel Compos. Struct., Int. J.*, **25**(3), 347-360.

Tahouneh, V. (2018), “3-D Vibration analysis of FG-MWCNTs/Phenolic sandwich sectorial plates”, *Steel Compos. Struct., Int. J.*, **26**(5), 649-662.

Tian, R. and Yagawa, G. (2007), “Allman’s triangle, rotational DOF and partition of unity”, *Int. J. Numer. Methods Eng.*, **69**(4), 837-858.

Tu, Z.-c. and Ou-Yang, Z.-c. (2002), “Single-walled and multiwalled carbon nanotubes viewed as elastic tubes with the effective Young’s moduli dependent on layer number”, *Phys. Review B*, **65**(23), 233407.

Valentini, L., Biagiotti, J., Kenny, J.M. and López Manchado, M.A. (2003), “Physical and mechanical behavior of single-walled carbon nanotube/polypropylene/ethylene–propylene–diene rubber nanocomposites”, *J. Appl. Polym. Sci.*, **89**(10), 2657-2663.

Vodenitcharova, T. and Zhang, L. (2006), “Bending and local buckling of a nanocomposite beam reinforced by a single-walled carbon nanotube”, *Int. J. Solids Struct.*, **43**(10), 3006-3024.

Wan, H., Delale, F. and Shen, L. (2005), “Effect of CNT length and CNT-matrix interphase in carbon nanotube (CNT) reinforced composites”, *Mech. Res. Commun.*, **32**(5), 481-489.

Wattanasakulpong, N. and Ungbhakorn, V. (2013), “Analytical solutions for bending, buckling and vibration responses of carbon nanotube-reinforced composite beams resting on elastic foundation”, *Computat. Mater. Sci.*, **71**, 201-208.

Weaver, Jr. W., Timoshenko, S.P. and Young, D.H. (1990). *Vibration Problems in Engineering*, John Wiley & Sons.

Wielentejczyk, P. and Lewandowski, R. (2017), “Geometrically nonlinear, steady state vibration of viscoelastic beams”, *Int. J. Non-Linear Mech.*, **89**, 177-186.

Yang, F., Sedaghati, R. and Esmailzadeh, E. (2008), “Free in-plane vibration of general curved beams using finite element method”, *J. Sound Vib.*, **318**(4-5), 850-867.

Yas, M. and Samadi, N. (2012), “Free vibrations and buckling analysis of carbon nanotube-reinforced composite Timoshenko beams on elastic foundation”, *Int. J. Pressure Vessels Piping*, **98**, 119-128.

Yazdani Sarvestani, H. and Ghayoor, H. (2016), “Free vibration analysis of curved nanotube structures”, *Int. J. Non-Linear Mech.*, **86**, 167-173.

Yu, Z., Guo, X. and Chu, F. (2010), “A multivariable hierarchical finite element for static and vibration analysis of beams”, *Finite Elem. Anal. Des.*, **46**(8),625-631.

Zhang, L. (2017), “On the study of the effect of in-plane forces on the frequency parameters of CNT-reinforced composite skew plates”, *Compos. Struct.*, **160**, 824-837.

Zhang, B. and Rajendran, S. (2008), “‘FE-Meshfree’QUAD4 element for free-vibration analysis”, *Comput. Methods Appl. Mech. Eng.*, **197**(45-48), 3595-3604.

Zhang, L., Song, Z. and Liew, K. (2015), “State-space Levy method for vibration analysis of FG-CNT composite plates subjected to in-plane loads based on higher-order shear deformation theory”, *Compos. Struct.*, **134**, 989-1003.

Zhong, H. and Guo, Q. (2003), “Nonlinear vibration analysis of Timoshenko beams using the Differential Quadrature Method”, *Nonlinear Dyn.*, **32**(3), 223-234.

Zhou, X., Huang, K. and Li, Z. (2018), “Geometrically nonlinear beam analysis of composite wind turbine blades based on quadrature element method”, *Int. J. Non-Linear Mech.*, **104**, 87-99.

CC